
Conformal Policy Control

Drew Prinster^{1,2} Clara Fannjiang¹ Ji Won Park¹ Kyunghyun Cho^{3,4} Anqi Liu² Suchi Saria²
Samuel Stanton⁴

Abstract

An agent must try new behaviors to explore and improve. In high-stakes environments, an agent that violates safety constraints may cause harm and must be taken offline, curtailing any future interaction. Imitating old behavior is safe, but excessive conservatism discourages exploration. How much behavior change is too much? We show how to use any safe reference policy as a probabilistic regulator for any optimized but untested policy. Conformal calibration on data from the safe policy determines how aggressively the new policy can act, while provably enforcing the user’s declared risk tolerance. Unlike conservative optimization methods, we do not assume the user has identified the correct model class nor tuned any hyperparameters. Unlike previous conformal methods, our theory provides finite-sample guarantees even for non-monotonic bounded constraint functions. Our experiments on applications ranging from natural language question answering to biomolecular engineering show that safe exploration is not only possible from the first moment of deployment, but can also improve performance.

1. Introduction

Safe exploration is one of the most studied problems in AI safety (Amodei et al., 2016). The choice between probable safety and the hope of possible discovery presents a dilemma known by many names, from the explore-exploit tradeoff in reinforcement learning to the validity-power tradeoff in statistics. The optimal balance is problem-dependent, yet general solutions must be problem-independent. Hence to apply to specific problems any general solution must encode this balance as a hyperparameter, which then must be tuned from data or derived from assumptions about problem

structure. In consequential settings, collecting data from an unsafe policy may be unacceptable. Deriving the balance from assumptions about the problem reintroduces a subtler form of problem-dependence, namely the practitioner’s understanding of the setting itself. Yet consequential, poorly understood settings are precisely where machine learning offers the greatest potential benefit.

Consider an agent that observes states, takes actions, and receives both rewards and constraint feedback. The agent’s goal is to maximize reward while respecting a risk tolerance, α . For example, a language model answering medical questions must avoid false claims, and a generative model proposing molecules must ensure they are synthesizable. A new policy has been optimized for performance but not yet tested. A safe policy already controls the risk, and instead of blindly deploying the untested policy, the agent can reuse its existing deployment data for calibration through importance weighting. The importance weights, however, depend on the deployed policy, and the deployed policy depends on the importance-weighted risk estimates. How should the agent proceed? Rather than assuming knowledge of the problem, we resolve this circularity by exploiting what the agent already knows about itself.

We introduce conformal policy control (CPC, Figure 1), a method for safe exploration that uses the calibration data to interpolate between any safe and any optimized policy while provably respecting the risk threshold. CPC requires no assumptions on the reward or constraint functions, no access to the optimized policy’s training process, and no additional samples to tune the balance beyond what a safe policy already provides. The key idea is to parameterize the balance as a likelihood-ratio threshold between the safe and optimized policies. Conformal calibration on the safe policy’s data determines the most aggressive threshold that still respects the declared risk. At deployment, the interpolated policy is realized through rejection sampling, which allows the agent to probabilistically self-regulate to a zone of competence determined by its calibration data. Because CPC operates entirely at test time, the same safe and optimized policies can be reused under different risk tolerances, trading test-time compute for risk control without retraining.

Providing finite-sample guarantees in this setting poses sev-

¹Prescient Design, Genentech, U.S.A. ²Johns Hopkins University, Baltimore, U.S.A. ³New York University, NYC, U.S.A. ⁴Formerly Prescient Design, Genentech. Correspondence to: Drew Prinster <drewprinster@gmail.com>, Samuel Stanton <sdstanton1@gmail.com>.

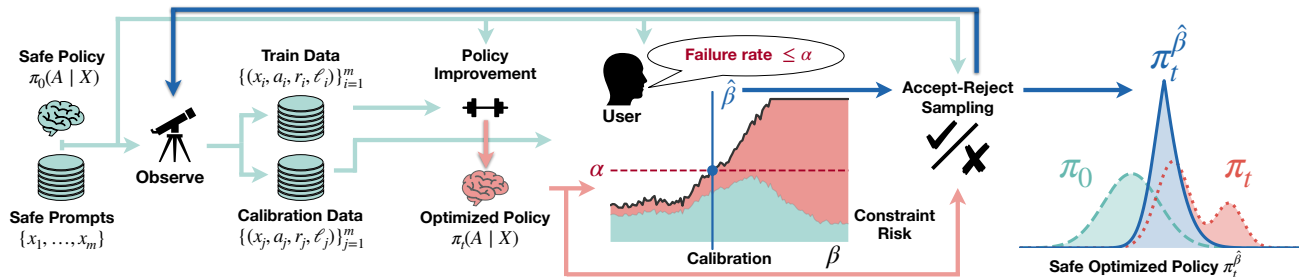


Figure 1. An illustration of safe exploration with conformal policy control. Starting with a safe policy π_0 and safe context prompts $\mathcal{X}_0 := \{x_1, \dots, x_m\}$, we observe the safe policy’s actions a_i and corresponding reward $r_i \in \mathbb{R}$ and constraint violation $\ell_i \in \{0, 1\}$. We split the observations into train and calibration data, and optimize the safe policy to obtain π_t . We then query the user for their constraint violation risk tolerance α , and apply conformal risk control to find a bound on the likelihood ratio π_t/π_0 which guarantees the calibrated risk is controlled at level α . Finally we apply rejection sampling to probabilistically regulate the optimized policy for deployment and observation, allowing the user to flexibly trade off reward, constraint risk, and test-time compute.

eral challenges for uncertainty quantification. The deployed policy depends on the calibration data, introducing subtle, data-dependent distribution shift. The relevant losses are general constraint functions, not just coverage indicators. Conformal risk control (CRC) (Angelopoulos et al., 2024) addresses both of these challenges, but assumes a monotone relationship between the control parameter and the loss. In CPC, the constraint function does not depend on the control parameter, so the monotonicity assumption does not hold. We extend CRC to non-monotonic bounded loss functions, and we prove that CPC inherits finite-sample guarantees when the control parameter governs the policy, not the loss.

We validate our method on three tasks. In medical question answering, we control the false discovery rate, a non-monotonic loss that standard CRC cannot handle directly. In constrained active learning, the agent’s actions induce feedback-loop shifts that violate standard exchangeability assumptions. In black-box sequence optimization, a language model agent must improve biomolecular sequences while respecting a constraint budget. In each setting, CPC provides finite-sample risk control from the first round of deployment, without hyperparameter tuning or structural assumptions. In medical question answering, this yields tighter risk control and better claim recall than existing methods. In active learning, we obtain finite-sample guarantees where previous approaches provide only asymptotic control. In sequence optimization, we extend conformal methods to a setting where no prior guarantees existed, and find that moderate risk control can counterintuitively improve optimization performance by stabilizing the algorithm. Safe exploration is not only safe, it can also be more efficient.

2. Background

We consider a decision-making agent that interacts with an environment over a sequence of rounds. At each round t , the agent observes a context (i.e., prompt) $X_t \in \mathcal{X}$ and selects an action $A_t \in \mathcal{A}$ according to a policy $\pi(A | X)$. If the

policy is parameterized by an LLM, then $\mathcal{A} \subseteq \mathcal{X}$. The agent then observes (potentially noisy) rewards $R_t \in \mathbb{R}$ and losses $L_t \in \mathbb{R}$. The reward function $r(x, a)$ quantifies the degree to which a context-action pair is aligned with the agent’s objective, and the loss function $\ell(x, a)$ quantifies whether the context-action pair satisfies the agent’s constraints. While a policy can be defined implicitly by solving an optimization problem with respect to estimated reward and loss surrogates (Watkins & Dayan, 1992; Jones et al., 1998), in this paper we focus on controlling explicit policies parameterized by a conditional distribution (Williams, 1992), such as an autoregressive transformer.

2.1. The Safe Policy Improvement Problem

The setting just introduced provides a general framework for sequential decision making under uncertainty (Langford & Zhang, 2008), capturing many problems of practical interest (Li et al., 2010). In natural language question answering (Rajpurkar et al., 2016), the context could be a user query, the action a generated response, and the reward and loss could reflect response completeness and (in)correctness, respectively. In constrained black-box optimization (Gardner et al., 2014), the context could be the previous evaluations, the action the next solution to evaluate, and the reward and loss functions could be black-box oracle objective and constraint functions, respectively (Chen et al., 2025). For example, in protein engineering, the loss function may indicate whether a proposed sequence lies outside a feasibility set \mathcal{F} of expressible proteins, i.e., $\ell(X_t, A_t) := \mathbb{1}\{A_t \notin \mathcal{F}\}$.

The agent’s goal is to learn a policy that maximizes expected reward while controlling expected loss. Formally, the agent seeks a policy π that solves

$$\begin{aligned} \max_{\pi} \quad & \mathbb{E}_{X \sim p} \mathbb{E}_{A \sim \pi(\cdot | X)} [r(X, A)] \\ \text{subject to} \quad & \mathbb{E}_{X \sim p} \mathbb{E}_{A \sim \pi(\cdot | X)} [\ell(X, A)] \leq \alpha, \end{aligned} \quad (1)$$

where $\alpha \in [0, B]$ (for some $B < \infty$) is a user-specified risk

tolerance, and $p(X)$ is the marginal context distribution.¹

In practice, the agent usually begins with a safe reference policy π_0 , whether inherited from a prior deployment or trained as a density model of known safe actions, and seeks to improve upon it. In the LLM literature, policy improvement is also known as post-training and encompasses methods such as supervised fine-tuning (SFT; Wei et al., 2022), reinforcement learning with human feedback (RLHF; Christiano et al., 2017) or direct preference optimization (DPO; Rafailov et al., 2023). The quality of the improved policy depends on the post-training dataset, the fidelity of any reward or preference models, and design decisions governing how far the policy may diverge from the safe reference.

Post-training design decisions immediately prompt two questions: which policy divergence measure is best, and how much divergence is allowable to maintain an acceptable risk profile? The first question has been studied extensively (see Section 3). The second, however, is typically treated as a hyperparameter tuning problem (Bergstra et al., 2011; Feurer & Hutter, 2019), in which the user must specify a constraint on a “control parameter”—such as a divergence budget or penalty weight—and the algorithm optimizes subject to that constraint. The resulting indirection creates a gap between what the user actually wants and the control parameters that are accessible in available algorithms (Hutchins et al., 1986; Norman, 1988). The user’s goal is declarative (i.e., a desired outcome of the program): control risk at some level α . The algorithms demand imperative instructions (i.e., the steps the program should execute): bound divergence at some level, or set the penalty weight to some value. Without a principled translation, the user must learn the mapping from outcome to instruction by trial and error, spending the very samples the agent seeks to use efficiently.

2.2. Conformal Risk Control

Ideally, the user would specify a risk threshold α and the algorithm would automatically determine the corresponding policy constraint. Conformal risk control (CRC; Angelopoulos et al., 2024) provides exactly this capability, but for a restricted class of problems. While CRC does not directly solve the policy control problem described above, it provides foundational ideas we build upon.

CRC is a framework for setting a control parameter in a way that controls the expected value of a user-specified loss function with finite-sample guarantees. The key assumptions are that the calibration loss functions L_1, \dots, L_n and test loss L_{n+1} are exchangeable, and that each loss function $L(\lambda)$ is monotonically nonincreasing with the control parameter λ . CRC selects $\hat{\lambda}$ to be the smallest value such that the empirical risk on the calibration data falls below the

target level adjusted by a finite-sample correction, which enables the guarantee $\mathbb{E}[L_{n+1}(\hat{\lambda})] \leq \alpha$. Conformal prediction (Vovk et al., 2005) is recovered as a special case when the loss is the miscalibration indicator $L(\lambda) = \mathbb{1}\{Y \notin \hat{C}_\lambda(X)\}$ for labels Y and prediction sets \hat{C}_λ , where the control parameter λ controls the size of the prediction set. When the calibration and test distributions differ, weighted conformal methods (Tibshirani et al., 2019) can be used to restore validity by reweighting the empirical risk according to the likelihood ratio $p_{\text{test}}/p_{\text{cal}}$.

The primary limitation of CRC for policy optimization is that the loss function must be monotonically nonincreasing with a tunable control parameter λ . Many losses of practical interest, such as indicators of violating feasibility/safety sets, cannot be parameterized in this way—unlike in the case of conformal prediction described above, where one can set the size of the prediction set to modulate the loss value, feasibility/safety sets are typically fixed. Our approach addresses this limitation by introducing the control parameter in the policy or data distribution that the expectation is taken over, rather than in the loss function. Even with this modification, the resulting expected loss is not necessarily monotonic in the control parameter, which presents a theoretical challenge we discuss further in Section 4.

3. Abbreviated Related Work

Conservative model-based optimization: A standard approach to safe policy improvement relies on the observation that the risk of a new policy can be bounded in terms of the risk of a reference policy plus a penalty that grows with the divergence between them (Kakade & Langford, 2002). When the reference policy is known to satisfy the safety constraint, controlling this divergence provides a mechanism for controlling risk. The idea of bounding risk through bounded divergence motivates a broad family of locality-constrained policy optimization methods (Kim et al., 2025). Prior work has proposed entropy-regularized control and KL-penalized objectives (Todorov, 2009; Fox et al., 2016), trust-region policy optimization (Schulman et al., 2015; 2017), conservative value penalties in offline reinforcement learning (Kumar et al., 2020; Trabucco et al., 2021), trust-region methods in black-box optimization (Eriksson et al., 2019), and uncertainty-penalized safe Bayesian optimization (Sui et al., 2015). Damani et al. (2023) proposed using a likelihood ratio as a safety filter for model-based optimization, but treated the likelihood ratio threshold as a hyperparameter for empirical tuning.²

From an optimization perspective, our work is most simi-

²Bounding the likelihood ratio $\pi_t(a | x)/\pi_0(a | x) \leq \beta$ uniformly implies a bound on the KL divergence and other f -divergences between π_t and π_0 . In this sense, likelihood ratio clipping is a strict form of divergence constraint.

¹In constrained optimization notation, r and ℓ map to f and g .

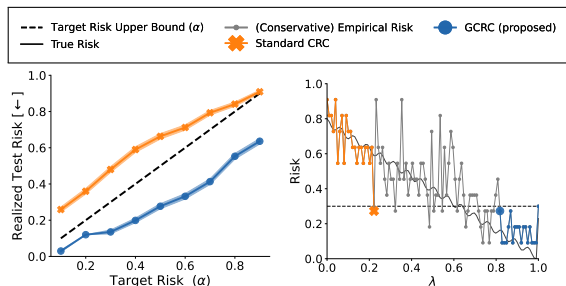


Figure 2. Empirical comparison of standard CRC (Angelopoulos et al., 2024) (orange) and the proposed generalized CRC (blue) on synthetic non-monotonic losses. gCRC achieves risk control across various target risk levels while CRC does not (left). On an example empirical risk trajectory for these experiments, CRC underestimates the risk while gCRC maintains risk control by searching from safe to aggressive hyperparameter values (right).

lar to Stanton et al. (2023), who proposed constraining a Bayesian optimization policy to regions where the resulting conformal prediction sets would have bounded width given a declarative miscoverage tolerance α . However, their approach was limited by three weaknesses. First, their approach was restricted to controlling the miscoverage loss. Second, their use of an implicit policy created an awkward fixed-point problem: finding the policy that induced an action distribution under which the coverage would be controlled at the desired level. Third, they did not fully address the multi-step feedback covariate shift induced by sequential model-based optimization.³ Indeed, Stanton et al. (2023) noted that, at the time, the existing conformal theory had not yet proved general enough guarantees to cover the multi-round model-based optimization setting.

Conformal methods: Stanton et al. (2023) drew motivation from Fannjiang et al. (2022), who first formalized the phenomenon of *feedback covariate shift* to generalize conformal prediction to the setting of a single round of model-based optimization, building on techniques introduced by Tibshirani et al. (2019). Prinster et al. (2024) further extended these techniques to generalize conformal prediction for any data distribution, including showing coverage guarantees for the multi-round model-based optimization setting.

However, the techniques used throughout this line of work do not enable one to prescribe a data distribution—e.g., select a policy—that guarantees coverage. That is, these methods can provide prediction sets with coverage guarantees for actions generated by any *fixed* policy (a “descriptive” use of conformal techniques), but using those prediction sets to then *select* a policy (a “prescriptive” use) introduces further, unaccounted-for dependence between the observed data and test policy that nullifies coverage guarantees.

³A form of covariate shift in which the test distribution is dependent on previously observed data.

To enable this prescriptive use case, we build upon techniques from conformal risk control (CRC) (Angelopoulos et al., 2024), a general framework for selecting a hyperparameter with finite-sample guarantees for any monotonic loss, of which conformal prediction can be cast as a special case. When the loss of interest is non-monotonic, Angelopoulos et al. (2024) also showed that deploying the procedure on a monotonic relaxation of the losses provides asymptotic guarantees of control. However, they left the problem of finite-sample guarantees for non-monotonic losses open. In the next section, we develop a variant of CRC that drops the monotonicity requirement, and instead relies on smoothness and a form of stability of the losses to control the risk on the test point. Finally, we apply techniques from Prinster et al. (2024) to prove finite-sample guarantees for our procedure in the multi-round model-based optimization setting. See Appendix A for an extended discussion of related work.

Concurrently with this paper, Angelopoulos (2026) also presents CRC guarantees for non-monotonic losses. A primary difference is that paper studies parameterized losses, whereas our paper introduces and focuses on policy control, where the control parameter tunes the policy rather than the loss. Even in the comparable setting of parameterized losses, however, the contributions are distinct, with neither subsuming the other: Relative to the univariate method in Angelopoulos (2026), our method (Section 4.1) will always be at least as a-priori conservative (e.g., as in Figure 2, right); consequently, whereas that paper’s analogous guarantee relies on leave-one-out stability, our results use replace-one stability, which is generally a more relaxed assumption (Bousquet & Elisseeff, 2002; Shalev-Shwartz et al., 2010).

4. Methods and Theory

4.1. Extending Conformal Risk Control to Non-Monotonic Losses

We begin with intuition. Standard CRC’s proof (Angelopoulos et al., 2024) has two key steps: First, prove that the oracle solution (using knowledge of the test point’s loss), λ^* , achieves risk control; and second, show that the empirical CRC solution (with a conservative adjustment for the unknown test loss), $\hat{\lambda}$, is deterministically greater than or equal to the oracle, $\hat{\lambda} \geq \lambda^*$. Note that here, larger λ are safer. In particular, for standard CRC, monotonicity of the loss function is then necessary and sufficient⁴ for concluding that the empirical CRC algorithm’s risk is controlled: $\mathbb{E}[L_{n+1}(\hat{\lambda})] \leq \mathbb{E}[L_{n+1}(\lambda^*)] \leq \alpha$.

Without monotonicity, what can be done? The crux is how to find a modified oracle solution, λ^*_+ , and a modified em-

⁴Sufficient given the other CRC assumptions: boundedness and right-continuity of the loss, and existence of a safe λ_{\max} .

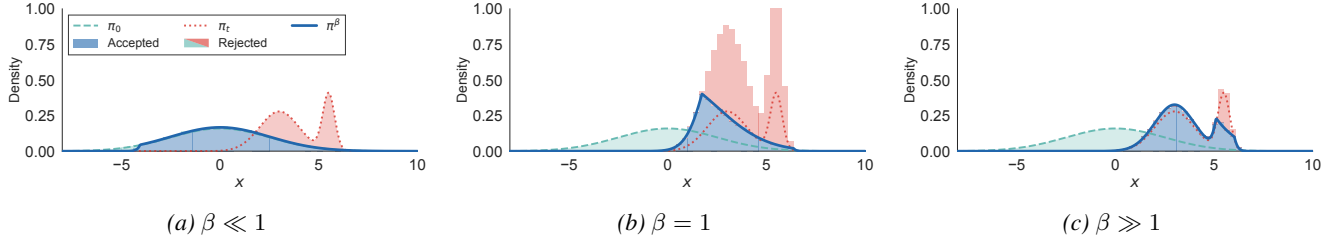


Figure 3. Rejection sampling for policy interpolation at three β values. As β increases from near-zero to large values, the constrained policy π^β interpolates from the safe policy π_0 to the optimized policy π_t . Blue histogram bars show accepted samples matching π^β , while teal/red bars show rejected samples from the proposal distribution. (a) Small β nearly recovers the safe policy (b) Intermediate β shows intermediate interpolation with frequent rejections. (c) Large β approaches the optimized policy with minimal rejection.

pirical algorithm, $\hat{\lambda}_+$, such that establishing the relation $\hat{\lambda}_+ \geq \lambda_+^*$ enables analyzing the risk of the empirical algorithm *by construction*, rather than by monotonicity. Consider the family of hyperparameters defined as

$$\begin{aligned} \hat{\lambda}_+(\mathcal{L}_{1:m}, \alpha) & \\ := \inf \left\{ \lambda_0 \in \Lambda : \forall \lambda \geq \lambda_0, \sum_{i=1}^m \frac{L_i(\lambda)}{m} \leq \alpha \right\}, & \end{aligned} \quad (2)$$

when the set is nonempty, and otherwise define $\hat{\lambda}_+(\mathcal{L}_{1:m}, \alpha) := \lambda_{\max}$, where a λ_{\max} is a “safe hyperparameter” that we assume exists as does Angelopoulos et al. (2024): $\lambda_{\max} := \sup \Lambda \in \Lambda$ and $L_i(\lambda_{\max}) \leq \alpha$. Note that $\hat{\lambda}_+(\mathcal{L}_{1:m}, \alpha)$ can roughly be interpreted as the smallest (most aggressive) hyperparameter such that the empirical risk, $\sum_{i=1}^m \frac{L_i(\lambda)}{m}$, is controlled at level α for all hyperparameters at least as large as it. That is, the “for all $\lambda \geq \lambda_0$ ” qualification in Eq. (2) is the key algorithmic modification to standard CRC. We then define the oracle solution by Eq. (2) fit on the bag (or multiset) containing both the calibration and test loss functions, $\mathcal{L}_{1:n+1}$:

$$\lambda_+^* := \hat{\lambda}_+(\mathcal{L}_{1:n+1}, \alpha). \quad (3)$$

Similarly, define the empirical algorithm as Eq. (2) fit on the bag of the calibration losses, with the bound B in place of L_{n+1} to conservatively adjust for the unknown test loss:

$$\hat{\lambda}_+ := \hat{\lambda}_+(\mathcal{L}_{1:n}, B, \alpha). \quad (4)$$

Our empirical algorithm, $\hat{\lambda}_+$, reduces to CRC when the losses are monotonic, and it can be viewed as searching hyperparameter space from *a priori* safest to most aggressive, the opposite direction of standard CRC (Figure 2). Also note that our generalized CRC (gCRC) is conservatively designed to be *a priori* safer than the oracle, that is, $\hat{\lambda}_+ \geq \lambda_+^*$ almost surely. Unfortunately, this construction is not itself sufficient for $\hat{\lambda}_+$ to achieve validity at level α (Appendix B.3). Relating the empirical algorithm to the oracle, however, does provide finite-sample guarantees for $\hat{\lambda}_+$ under Lipschitz continuity and depending on algorithmic stability.

Definition 4.1 (ϵ -replace-one stability). We say that a function h is ϵ -replace-one stable if for all $i, j \in [n+1]$,

$$\mathbb{E} \left[\left| h(\mathcal{Z}_{1:n+1 \setminus i}) - h(\mathcal{Z}_{1:n+1 \setminus j}) \right| \right] \leq \epsilon.$$

The following result then provides finite-sample guarantees for $\hat{\lambda}_+$ even for non-monotonic losses.

Theorem 4.2. Assume exchangeable $L_i(\lambda)$. Define $\lambda_{\max} := \sup \Lambda \in \Lambda$ and assume

$$L_i(\lambda_{\max}) \leq \alpha, \quad \sup_{\lambda} L_i(\lambda) \leq B < \infty \quad \text{almost surely.}$$

If the $L_i(\lambda)$ are K -Lipschitz in λ and $\hat{\lambda}_+$ is ϵ -replace-one stable, then

$$\mathbb{E}[L_{n+1}(\hat{\lambda}_+)] \leq \alpha + K\epsilon.$$

Proof sketch: Conditional on the bag of data, $\mathcal{Z}_{1:n+1}$, we show that the oracle λ_+^* achieves risk control, which implies risk control for all $\lambda \geq \lambda_+^*$ that are constant conditional on $\mathcal{Z}_{1:n+1}$. We then show $\hat{\lambda}_+ \geq \lambda_+^*$ almost surely. Lastly, using Lipschitz continuity and replace-one stability, we relate the risk of $\hat{\lambda}_+$ to that of some $\lambda \geq \lambda_+^*$ that is constant conditional on $\mathcal{Z}_{1:n+1}$. We defer the proof to App. B.1.

Remark 4.3 (Attaining α -validity if K is known). If K is known, then a more conservative significance level, $\hat{\alpha} \leq \alpha$, can be used for level α validity, regardless of instability:

$$\mathbb{E}[L_{n+1}(\hat{\lambda}_+(\hat{\alpha}))] \leq \alpha,$$

where $\hat{\alpha}$ is defined in Appendix B.4.

Remark 4.4 (Monotone envelope interpretation). The $\hat{\lambda}_+$ in Eq. (4) can be viewed as the smallest hyperparameter such that the “monotized empirical risk” is controlled at α . The procedure is presented with this interpretation in Angelopoulos et al. (2024)’s App. A, but that paper noted that finite-sample guarantees for $\hat{\lambda}_+$ were at the time unknown.

Algorithm 1 Pseudo-code for β calibration.

Require: Safe policy π_0 ; optimized policies π_1, \dots, π_t ; sets of prompts $X^{(0)}, \dots, X^{(t)}$; calibration data \mathcal{D}_{cal} ; proposal data $\mathcal{D}_{\text{prop}} \sim \pi_t$; target risk α ; loss upper bound B .

Ensure: Likelihood ratio bound $\hat{\beta}$

$\rho_i \leftarrow \pi_t(A_i | X^{(t)}) / \pi_0(A_i | X^{(0)})$ for $i \in \mathcal{D}_{\text{cal}} \cup \mathcal{D}_{\text{prop}}$

$G \leftarrow \text{PREPAREGRID}(\{\rho_i\})$

Initialize: $\hat{\beta} \leftarrow \beta_{\min}$

for $\beta \in G$ (ascending) **do**

 # Compute constrained PDF, mixture of past PDFs

$\psi_\beta \leftarrow \text{ESTIMATEPSI}(\{\rho_i\}, \beta)$

$\pi_t^{(\beta)}(A_i) \leftarrow \min(\rho_i, \beta) / \psi_\beta$ for $i \in \mathcal{D}_{\text{cal}}$

$\pi_{0:t-1}^{\text{mix}}(A_i) \leftarrow \text{MIXPDF}(A_i, \pi_{0:t-1})$ for $i \in \mathcal{D}_{\text{cal}}$

 # Compute conformal weights, check empirical risk

$w_i \leftarrow \pi_t^{(\beta)}(A_i) / \pi_{0:t-1}^{\text{mix}}(A_i)$ for $i \in \mathcal{D}_{\text{cal}}$

$w_{\max} \leftarrow \text{ESTIMATEWMAX}(\{w_i\}, \pi_0, \pi_t)$

$\tilde{w}_i \leftarrow w_i / (\sum_{j \in \mathcal{D}_{\text{cal}}} w_j + w_{\max})$ for $i \in \mathcal{D}_{\text{cal}}$

if $\sum_{i \in \mathcal{D}_{\text{cal}}} \tilde{w}_i \cdot L_i + \tilde{w}_{\max} \cdot B > \alpha$ **then**

Return: $\hat{\beta}$

end if

$\hat{\beta} \leftarrow \beta$

end for

Return: $+\infty$

4.2. Conformal Policy Control: Selecting a Risk-Controlling Policy

We first state the only critical assumptions required by CPC: access to a safe policy and subsequent optimized policies. For ease of notation we will describe CPC in an online setting where one action is taken or sample generated each policy improvement step, but it also works similarly in a multiround batch setting.

Assumption 1: An Initial Safe Policy Assume access to an initial safe policy, π_0 , for which the true risk is controlled at the desired level α ; that is, assume $\mathbb{E}_{X \sim p} \mathbb{E}_{A \sim \pi_0(\cdot | X)} [\ell(X, A)] \leq \alpha$ holds for π_0 .

Assumption 2: Access to Each Optimized Policy At each time $t = 1, 2, \dots$, also assume access to the optimized model, π_t , which may be trained to maximize expected reward (as in the “unconstrained” part of Eq. (1)). We do not require any assumptions on how π_t is trained, although better optimized performance (with respect to both the constraint and the reward) may translate into better efficiency and reward of the constrained policy.

Constraining Policies by Clipping Likelihood Ratios We define the constrained policy $\pi_t^{(\beta)}$ by clipping the likelihood ratio π_t / π_0 at a bound $\beta > 0$ and renormalizing. Actions whose likelihood ratio exceeds β are capped at $\beta \cdot \pi_0$, limiting how far the constrained policy can deviate from the safe

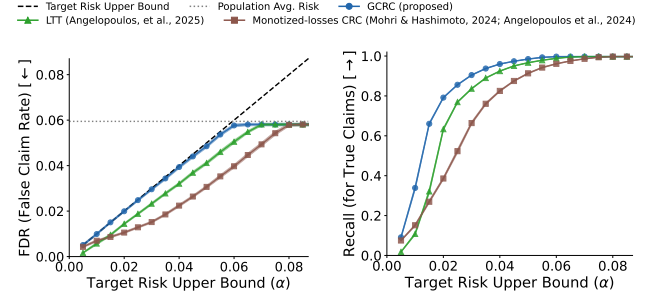


Figure 4. Medical QA factuality control results on MedLFQA. **Left:** Empirical FDR (fraction of retained claims that are false) vs. target risk level α . The dashed line indicates $y = x$; valid methods should fall at or below this line. **Right:** Recall (fraction of true claims retained) vs. α . gCRC tightly controls FDR at the target level while achieving superior recall to baselines. Results averaged over 25 random splits. Error regions are standard errors.

policy. That is,

$$\pi_t^{(\beta)}(x) \propto \min(\pi_t(x), \beta \cdot \pi_0(x)). \quad (5)$$

Assume there is some small, positive $\beta_{\min} \ll 1$ such that $\beta_{\min} \leq \pi_t(x) / \pi_0(x)$ for all $x \in \mathcal{X}$. Then, note that as $\beta \rightarrow \beta_{\min}$, the constrained policy approaches the safe one: $\pi_t^{(\beta)} \rightarrow \pi_0$. Also note that as $\beta \rightarrow \infty$, the constrained policy approaches the optimized: $\pi_t^{(\beta)} \rightarrow \pi_t$ (Figure 3).

Calibrating β : Like λ in Section 4.1, β is a control parameter, but it acts on the policy rather than the loss. We calibrate β as we fit $\hat{\lambda}_+$, by searching from what we *a priori* expect is safest to most aggressive. Here for β , this means searching in increasing order in a grid (or set of intervals) $G \subset (0, \infty]$, to find the largest value where the conservatively-adjusted weighted empirical risk is still controlled:

$$\hat{\beta}(\mathcal{L}_{0:t-1}, B, \{\tilde{w}_{0:t-1}^{(\cdot)}, \tilde{w}_{\max}^{(\cdot)}\}, \alpha) \quad (6)$$

$$:= \sup \left\{ \beta' \in G : \forall \beta \leq \beta', B \tilde{w}_{\max}^{(\beta)} + \sum_{i=0}^{t-1} l_i \tilde{w}_i^{(\beta)} \leq \alpha \right\},$$

where the $\tilde{w}_i^{(\beta)}$ and $\tilde{w}_{\max}^{(\beta)}$ are carefully constructed (normalized) conformal importance weights. That is, for our theory, we define $\tilde{w}_i^{(\beta)}$ as in Prinster et al. (2024) via computing the likelihoods of all permutations of the calibration data $z_{0:t-1}$ and a hypothetical test sample $z_t \in \mathcal{Z} := \mathcal{X} \times \mathcal{A}$, but a key subtlety here is that z_t is not yet known, as CPC calibration is prior to sampling. For any z_t , define unnormalized weight

$$w_i^{(\beta)} := \sum_{\sigma: \sigma(t)=i} \pi_{0:t}^{(\beta)}(z_{\sigma(0)}, \dots, z_{\sigma(t)})$$

for all $i \in \{0, \dots, t\}$ and for permutations σ of the indices. For $i \in \{0, \dots, t\}$, further denote the normalized weights as

$$\tilde{w}_i^{(\beta)} := w_i^{(\beta)} / \sum_{i=0}^t w_i^{(\beta)}$$

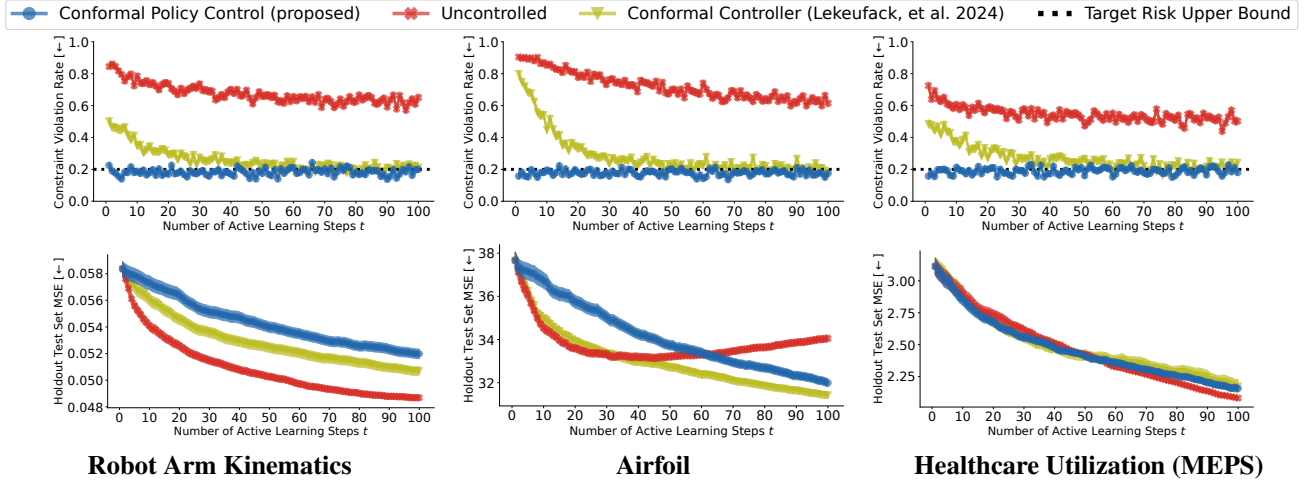


Figure 5. Conformal policy control in the active learning setting. We train Gaussian process regression models on tabular datasets, providing a small amount of initial data for training and selecting the remaining training data via exponential tilting toward the posterior predictive variance. We introduce a feasibility constraint based on alignment with the leading principal component of the Gram matrix to make the task more difficult. CPC controls the constraint violation risk at our desired threshold $\alpha = 0.2$, while simultaneously reducing test MSE. Surprisingly, in some cases the risk-controlled data selection policy attains lower test MSE than the uncontrolled policy.

and the conservative weight for an unknown test point as

$$\tilde{w}_{\max}^{(\beta)} := \sup_{z_t \in \mathcal{Z}} (\tilde{w}_t^{(\beta)}).$$

Hereon, we refer to normalized calibration and (conservative) test point weights, that is, assuming $\sum_{i=0}^{t-1} \tilde{w}_i^{(\beta)} + \tilde{w}_{\max}^{(\beta)} = 1$. In practice these weights are not computationally tractable, but we estimate the $\tilde{w}_i^{(\beta)}$ by approximating past policies as one mixture distribution, $\pi_{0:t-1}^{\text{mix}} \approx \pi_{0:t-1}$, which yields a fast linear runtime; additionally, we estimate $\tilde{w}_{\max}^{(\beta)}$ by an empirical maximum over samples from π_0 and π_t . If the weights are computed exactly, CPC achieves the following guarantee.

Theorem 4.5. *Assume that $\mathbb{E}_{\pi_0}[L_t] \leq \alpha$, $L_i \in [0, B]$, $B < \infty$ for all i , and $\hat{\beta}$ is ϵ -replace-one stable. If $w_i^{(\beta)}$ is K -Lipschitz in β for all i , then*

$$\mathbb{E}_{\pi_{0:t}^{(\hat{\beta})}}[L_t] \leq \alpha + BK\epsilon.$$

If $(l_i - \alpha) \cdot w_i^{(\beta)}$ is K' -Lipschitz in β , then

$$\mathbb{E}_{\pi_{0:t}^{(\hat{\beta})}}[L_t] \leq \alpha + K'\epsilon.$$

Note that unlike Theorem 4.2, where the Lipschitz condition is on $l_i(\lambda)$, here the Lipschitz condition is on $w_i^{(\beta)}$ or $(l_i - \alpha) \cdot w_i^{(\beta)}$ as a function of β . Since l_i does not depend on β , this regularity is determined entirely by the conformal weights, which depend on the likelihood ratio between the safe and optimized policies. The assumption thus concerns the agent’s own policies rather than the unknown constraint function.

Sampling from the Constrained Policy in Combinatorial Action Spaces

In large action spaces, the normalization constant of $\pi_t^{(\hat{\beta})}$ is intractable. However, accept-reject (AR) sampling (Von Neumann et al., 1963) avoids normalization entirely. When $\hat{\beta}$ is small, proposals from π_0 are efficient, with the AR envelope constant set to $\hat{\beta}$. When $\hat{\beta}$ is large, proposals from π_t are more efficient, since $\pi_t^{(\hat{\beta})} \approx \pi_t$. See Figure 3 and Appendix C.2 for details.

5. Experiments

We present three experiments. First, we apply generalized CRC (gCRC) to control the false discovery rate in medical question answering, a non-monotonic loss. Second, we apply CPC to constrained active learning, where feedback-loop shifts break exchangeability. Third, we apply CPC to black-box sequence optimization with a language model.

5.1. Factual Medical Question-Answering

Setup: We evaluate CRC methods on the MedLFQA dataset (Jeong et al., 2024), which aggregates medical question-answering benchmarks. We use the dataset of Cherian et al. (2024), which contains GPT-3.5-Turbo responses, atomic subclaims extracted via GPT-4o, and factuality annotations obtained by checking each subclaim against reference answers. Given a confidence score $p(C_{ij} | X_i)$ for each subclaim, we filter claims below a threshold τ and measure the false discovery rate (FDR), the fraction of retained claims that are false, as our loss. We measure recall, the fraction of total true claims retained, as our utility metric. Unlike the binary loss used by Mohri & Hashimoto (2024) and

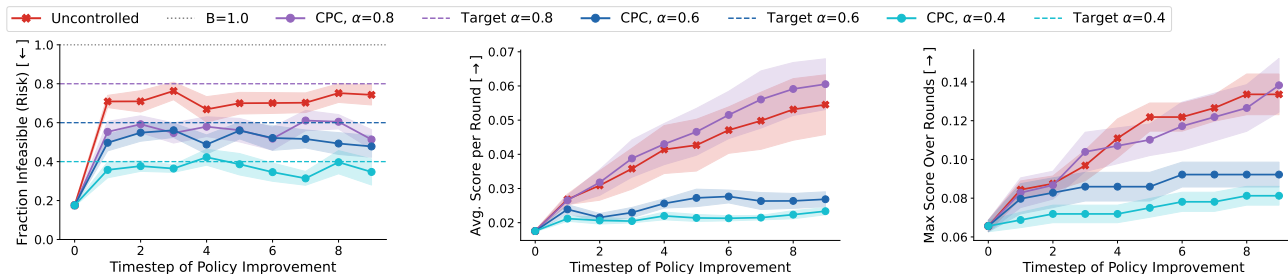


Figure 6. We apply CPC to constrained black-box sequence optimization scored with Ehrlich functions. **Left:** average infeasibility rate per round. **Center:** average objective value of sequences sampled from the policy. **Right:** best objective value found so far. CPC allows direct control over constraint violation risk via α . Without CPC, the infeasibility risk quickly rises to nearly 80% of policy samples. Moderate risk control ($\alpha > 0.6$) stabilizes optimization and improves overall performance by reducing wasted samples on infeasible actions.

Cherian et al. (2024), FDR is non-monotonic in τ , making it a natural test case for gCRC. We compare gCRC against monotonized-losses CRC and Learn Then Test (LTT) (Angelopoulos et al., 2025). See Appendix D for details.

Results: Figure 4 shows FDR and recall across varying risk levels α . gCRC controls FDR at or below the target level across all α values while achieving recall at least as high, or often significantly higher, than both the monotonized-losses CRC and LTT baselines. Relative to gCRC, the conservatism of LTT is due to its use of concentration inequalities for a high-probability guarantee, and that of monotonized-losses CRC is a consequence of Jensen’s inequality (monotonizing losses is far more conservative than monotonizing the empirical risk or average loss value). These results demonstrate that gCRC provides valid risk control for non-monotonic losses where standard CRC may not be valid, and empirically with higher power than baselines.

5.2. Constrained Active Learning

Setup: we evaluate CPC in a pool-based active learning setting on three regression datasets: **Robot Arm Kinematics**, **Airfoil**, and **Healthcare Utilization (MEPS)**. Starting from a small initial training set, the learner iteratively selects records from the pool to minimize test MSE. To create a challenging constrained setting, we construct synthetic feasibility constraints based on the first principal component of the covariate matrix. Records that follow the dominant covariation pattern (high PC1 values) are likely feasible, while records that deviate from this pattern are likely infeasible. Initial training data is sampled from the high-PC1 region, so the learner begins in a high-feasibility region. Uncertainty-based acquisition naturally targets the opposite end of the spectrum. We fit a Gaussian process regression model and define an acquisition policy via exponential tilting toward posterior variance: $\pi(a) \propto \exp(\lambda \cdot \hat{\sigma}_a^2)$. CPC constrains this policy relative to the source distribution used for initialization. See Appendix E for details.

Results: In Figure 5 we present results across all three

datasets. CPC successfully controls constraint violation risk at the target α while reducing test MSE. Surprisingly, in some cases the risk-controlled policy attains *lower* test MSE than the unconstrained policy, suggesting that avoiding infeasible regions improves sample efficiency.

5.3. Constrained Black-Box Optimization

Setup: Now consider a more difficult setting, black-box sequence optimization. Here, our goal is to identify a sequence of tokens $a \in \mathcal{X}$ to maximally improve the objective value of a current solution $x \in \mathcal{X}$. We evaluate on Ehrlich functions (Chen et al., 2025), synthetic test functions designed to capture the geometric structure of biomolecular sequence optimization problems. We use **Ehr(32, 32)-4-4-4**: sequences of length 32 over a vocabulary of size 32, with 4 motifs of length 4. We create an initial data package by running a genetic algorithm from a single feasible solution. We train π_{θ_0} by applying SFT to a Pythia 14M-parameter decoder-only transformer (Biderman et al., 2023) on improving pairs from the GA history. In later rounds, we sample from the current policy, collect oracle feedback, and fine-tune via DPO. CPC constrains each improved policy π_{θ_t} before sampling. See Appendix F for details.

Results: In Figure 6 we show that CPC effectively controls the risk of generating infeasible sequences while still improving the objective value over time. Again we find that moderate risk control ($\alpha > 0.6$) can produce controlled policies that slightly *outperform* their unconstrained counterparts, likely by wasting fewer evaluations on infeasible actions.

6. Discussion

We set out to resolve a circularity. The safe policy’s deployment data can be reweighted to estimate the risk of a new policy, but the correct weights depend on which policy is deployed, and the deployed policy depends on the weighted risk estimates. Conformal policy control resolves this by parameterizing the deployed policy as a likelihood-

ratio threshold, then calibrating that threshold on the safe policy’s data to find the most aggressive setting that still respects the risk threshold.

The guarantees we provide are marginal: risk is controlled on average over context and calibration data draws. This is the natural guarantee for deployment decisions, where one asks whether a policy is safe to deploy across a population. It is less informative for individual decisions, where one asks whether a particular action is safe for a particular context. Stronger conditional guarantees are possible but require additional assumptions or more conservative bounds (Thomas et al., 2019). Our guarantees also depend on the stability of the context distribution. If the context distribution begins to shift then recalibration may be necessary, or some risk control gap may need to be tolerated (Barber et al., 2023). Monitoring methods based on conformal martingales offer a principled approach to detecting such shifts (Prinster et al., 2025). We have also assumed the policy likelihoods are computable in closed form. If the policy likelihoods are intractable, then density ratio estimation (Sugiyama et al., 2012) or neural ratio estimation (Cranmer et al., 2020) techniques may be applicable.

Safety and exploration need not run counter to each other. In the right balance, they correct each other’s deficiencies, avoiding complacency on the one hand and dissipation on the other. However, it must be possible to determine an acceptable balance from what we actually know, not what we hope to be true. It can be enough, it turns out, to know what works, and to know what we want to do next.

Code Availability

Code to reproduce the results is available at <https://github.com/samuelstanton/conformal-policy-control>.

Broader Impact Statement

The dominant paradigm for deploying machine learning systems might be characterized as “train, deploy, and pray”. Collect data, train a model, tune hyperparameters until empirical performance seems acceptable, deploy, and hope that test-time behavior remains within tolerable bounds. When failures occur, the response is typically reactive, patching the system after harm has been observed. This paradigm persists not because practitioners prefer it, but because principled alternatives have been lacking.

This work contributes to a shift from safety-through-patching toward safety-by-design. Rather than discovering failure modes empirically and addressing them post-hoc, conformal policy control allows practitioners to specify acceptable risk levels before deployment and obtain guarantees that these levels will be respected. The hyperparameter tuning phase becomes about improving performance within safety constraints, rather than searching for a configuration that might satisfy unspecified feasibility requirements.

If such methods become widespread, the implications for where and how machine learning is deployed could be substantial. High-stakes domains that have resisted ML adoption due to liability concerns or regulatory barriers, such as clinical decision support, autonomous systems, and financial services, may become more accessible when developers can provide formal guarantees rather than empirical assurances. Such a change in framing would align ML deployment with the safety certification practices already standard in aviation, pharmaceuticals, and other regulated industries.

Acknowledgments

D.P, A.L., and S. Saria were partially funded by the Gordon and Betty Moore Foundation grant #12128. The authors would like to thank Hannah Lawrence and Neha Verma for helpful feedback.

References

Amodei, D., Olah, C., Steinhardt, J., Christiano, P., Schulman, J., and Mané, D. Concrete problems in AI safety. <https://arxiv.org/abs/1606.06565>, 2016.

Angelopoulos, A., Candès, E., and Tibshirani, R. J. Conformal PID control for time series prediction. In *Advances in Neural Information Processing Systems*, volume 36, pp. 23047–23074. Curran Associates, Inc., 2023.

Angelopoulos, A. N. Conformal risk control for non-monotonic losses, 2026. URL <https://arxiv.org/abs/2602.20151>.

Angelopoulos, A. N., Bates, S., Fisch, A., Lei, L., and Schuster, T. Conformal risk control. In *International Conference on Learning Representations*, 2024.

Angelopoulos, A. N., Bates, S., Candès, E. J., Jordan, M. I., and Lei, L. Learn then test: Calibrating predictive algorithms to achieve risk control. *Annals of Applied Statistics*, 19(2), 2025.

Bai, T. and Jin, Y. Optimized conformal selection: Powerful selective inference after conformity score optimization. [arXiv:2411.17983](https://arxiv.org/abs/2411.17983), November 2024.

Barber, R. F. and Tibshirani, R. J. Unifying different theories of conformal prediction. [arXiv preprint arXiv:2504.02292](https://arxiv.org/abs/2504.02292), 2025.

Barber, R. F., Candès, E. J., Ramdas, A., and Tibshirani, R. J. Predictive inference with the jackknife+. *The Annals of Statistics*, 49(1):486–507, 2021.

Barber, R. F., Candès, E. J., Ramdas, A., and Tibshirani, R. J. Conformal prediction beyond exchangeability. *Ann. Stat.*, 51(2):816–845, April 2023.

Bastani, O., Gupta, V., Jung, C., Noarov, G., Ramalingam, R., and Roth, A. Practical adversarial multivald conformal prediction. In *Advances in Neural Information Processing Systems*, volume 35, pp. 29362–29373. Curran Associates, Inc., 2022.

Bates, S., Angelopoulos, A., Lei, L., Malik, J., and Jordan, M. Distribution-free, risk-controlling prediction sets. *Journal of the ACM (JACM)*, 68(6):1–34, 2021.

Bergstra, J., Bardenet, R., Bengio, Y., and Kégl, B. Algorithms for hyper-parameter optimization. *Advances in neural information processing systems*, 24, 2011.

Berkenkamp, F., Schoellig, A. P., and Krause, A. Safe controller optimization for quadrotors with gaussian processes. In *2016 IEEE international conference on robotics and automation (ICRA)*, pp. 491–496. Ieee, 2016.

Berkenkamp, F., Krause, A., and Schoellig, A. P. Bayesian optimization with safety constraints: safe and automatic parameter tuning in robotics. *Machine learning*, 112(10): 3713–3747, 2023.

Biderman, S., Schoelkopf, H., Anthony, Q., Bradley, H., O’Brien, K., Hallahan, E., Khan, M. A., Purohit, S., Prashanth, U. S., Raff, E., Skowron, A., Sutawika, L., and van der Wal, O. Pythia: A suite for analyzing large language models across training and scaling. In *International*

- Conference on Machine Learning, pp. 2397–2430. Pmlr, 2023.
- Bousquet, O. and Elisseeff, A. Stability and generalization. Journal of machine learning research, 2(Mar):499–526, 2002.
- Brooks, T. F., Pope, D. S., and Marcolini, M. A. Airfoil self-noise and prediction. Technical Report Rp-1218, Nasa, July 1989.
- Chandak, Y., Jordan, S., Theodorou, G., White, M., and Thomas, P. S. Towards safe policy improvement for non-stationary MDPs. In Advances in Neural Information Processing Systems, volume 33, 2020.
- Chen, A., Stanton, S. D., Ding, F., Alberstein, R. G., Watkins, A. M., Bonneau, R., Gligorijevic, V., Cho, K., and Frey, N. C. Generalists vs. specialists: Evaluating llms on highly-constrained biophysical sequence optimization tasks. In Forty-second International Conference on Machine Learning, 2025.
- Cherian, J., Gibbs, I., and Candes, E. Large language model validity via enhanced conformal prediction methods. Advances in Neural Information Processing Systems, 37: 114812–114842, 2024.
- Christiano, P. F., Leike, J., Brown, T. B., Martic, M., Legg, S., and Amodei, D. Deep reinforcement learning from human preferences. In Advances in Neural Information Processing Systems, volume 30, pp. 4299–4307, 2017.
- Colombo, N. and Vovk, V. Training conformal predictors. In Conformal and Probabilistic Prediction and Applications, pp. 55–64. Pmlr, 2020.
- Correia, A. H. C. and Louizos, C. Non-exchangeable conformal prediction with optimal transport: Tackling distribution shifts with unlabeled data. In Advances in Neural Information Processing Systems, volume 39, 2025.
- Cortes-Gomez, S., Patino, C., Byun, Y., Wu, S., Horvitz, E., and Wilder, B. Utility-directed conformal prediction: A decision-aware framework for actionable uncertainty quantification. International Conference on Learning Representations, 2025.
- Cranmer, K., Brehmer, J., and Louppe, G. The frontier of simulation-based inference. Proceedings of the National Academy of Sciences, 117(48):30055–30062, 2020.
- Cresswell, J. C., Sui, Y., Kumar, B., and Vouitsis, N. Conformal prediction sets improve human decision making. arXiv preprint arXiv:2401.13744, 2024.
- Damani, F., Brookes, D. H., Sternlieb, T., Webster, C., Malina, S., Jajoo, R., Lin, K., and Sinai, S. Beyond the training set: An intuitive method for detecting distribution shift in model-based optimization. arXiv preprint arXiv:2311.05363, 2023.
- De Santi, R., Vlastelica, M., Hsieh, Y.-P., Shen, Z., He, N., and Krause, A. Flow density control: Generative optimization beyond entropy-regularized fine-tuning. NeurIPS, 2025.
- Domingo-Enrich, C., Drozdal, M., Karrer, B., and Chen, R. T. Q. Adjoint matching: Fine-tuning flow and diffusion generative models with memoryless stochastic optimal control. In International Conference on Learning Representations, 2025.
- Eriksson, D., Pearce, M., Gardner, J., Turner, R., and Poloczek, M. Scalable global optimization via local bayesian optimization. In Advances in Neural Information Processing Systems, volume 32, 2019.
- Ezzati-Rice, T. M., Rohde, F., and Greenblatt, J. Sample design of the Medical Expenditure Panel Survey household component, 1998-2007. US Department of Health & Human Services, Agency for Healthcare Research and . . . , 2008.
- Fannjiang, C. and Park, J. W. Reliable algorithm selection for machine learning-guided design. In Singh, A., Fazel, M., Hsu, D., Lacoste-Julien, S., Berkenkamp, F., Maharaj, T., Wagstaff, K., and Zhu, J. (eds.), Proceedings of the 42nd International Conference on Machine Learning, volume 267 of Proceedings of Machine Learning Research, pp. 16078–16101. Pmlr, 13–19 Jul 2025.
- Fannjiang, C., Bates, S., Angelopoulos, A. N., Listgarten, J., and Jordan, M. I. Conformal prediction under feedback covariate shift for biomolecular design. Proceedings of the National Academy of Sciences, 119 (43):e2204569119, 2022.
- Feldman, S., Ringel, L., Bates, S., and Romano, Y. Achieving risk control in online learning settings. Transactions on Machine Learning Research, 2023. ISSN 2835-8856.
- Feurer, M. and Hutter, F. Hyperparameter optimization. In Automated machine learning: Methods, systems, challenges, pp. 3–33. Springer International Publishing Cham, 2019.
- Fox, R., Pakman, A., and Tishby, N. Taming the noise in reinforcement learning via soft updates. In Proceedings of the 32nd Conference on Uncertainty in Artificial Intelligence, pp. 202–211, 2016.
- Gardner, J. R., Kusner, M. J., Xu, Z. E., Weinberger, K. Q., and Cunningham, J. P. Bayesian optimization with inequality constraints. In Proceedings of the 31st

- International Conference on Machine Learning, pp. 937–945, 2014.
- Gibbs, I. and Candes, E. Adaptive conformal inference under distribution shift. Adv. Neural Inf. Process. Syst., 34:1660–1672, 2021.
- Giguere, S., Metevier, B., Castro da Silva, B., Brun, Y., Thomas, P. S., and Niekum, S. Fairness guarantees under demographic shift. In International Conference on Learning Representations, 2022.
- Gui, Y., Jin, Y., Nair, Y., and Ren, Z. Acs: An interactive framework for conformal selection, 2025. URL <https://arxiv.org/abs/2507.15825>.
- Hastings, W. K. Monte carlo sampling methods using markov chains and their applications. Biometrika, 57(1):97, 1970.
- Hoff, P. Bayes-optimal prediction with frequentist coverage control. Bernoulli, 29(2):901–928, 2023.
- Hullman, J., Wu, Y., Xie, D., Guo, Z., and Gelman, A. Conformal prediction and human decision making. arXiv preprint arXiv:2503.11709, 2025.
- Hutchins, E. L., Hollan, J. D., and Norman, D. A. Direct manipulation interfaces. In Norman, D. A. and Draper, S. W. (eds.), User Centered System Design: New Perspectives on Human-Computer Interaction, pp. 87–124. Lawrence Erlbaum Associates, 1986.
- Jeong, M., Hwang, H., Yoon, C., Lee, T., and Kang, J. OLAPH: Improving factuality in biomedical long-form question answering. arXiv preprint arXiv:2405.12701, 2024.
- Jiang, Z., Liu, A., and Van Durme, B. Conformal linguistic calibration: Trading-off between factuality and specificity. arXiv preprint arXiv:2502.19110, 2025.
- Jin, Y. and Candès, E. Selection by prediction with conformal p-values. J. Mach. Learn. Res., 24(244):244:1–244:41, October 2022.
- Jin, Y. and Candès, E. J. Model-free selective inference under covariate shift via weighted conformal p-values. Biometrika, 2025. doi: 10.1093/biomet/asaf066. Advance article.
- Jones, D. R., Schonlau, M., and Welch, W. J. Efficient global optimization of expensive black-box functions. Journal of Global optimization, 13(4):455–492, 1998.
- Jonkers, J., Van Wallendael, G., Duchateau, L., and Van Hoecke, S. Conformal predictive systems under covariate shift. Conformal and Probabilistic Prediction with Applications, 2024.
- Kakade, S. and Langford, J. Approximately optimal approximate reinforcement learning. In Proceedings of the Nineteenth International Conference on Machine Learning, pp. 267–274, 2002.
- Kappen, H. J. Path integrals and symmetry breaking for optimal control theory. Journal of statistical mechanics: theory and experiment, 2005(11):P11011, 2005.
- Kim, M., Gu, J., Yuan, Y., Yun, T., Liu, Z., Bengio, Y., and Chen, C. Offline model-based optimization: Comprehensive review. arXiv preprint arXiv:2503.17286, 2025.
- Kirschner, J., Mutny, M., Hiller, N., Ischebeck, R., and Krause, A. Adaptive and safe bayesian optimization in high dimensions via one-dimensional subspaces. In International Conference on Machine Learning, pp. 3429–3438. Pmlr, 2019.
- Kiyani, S., Pappas, G. J., Roth, A., and Hassani, H. Decision theoretic foundations for conformal prediction: Optimal uncertainty quantification for risk-averse agents. In Proceedings of the 42nd International Conference on Machine Learning, volume 267 of Proceedings of Machine Learning Research, pp. 30943–30965. Pmlr, 2025.
- Kumar, A., Zhou, A., Tucker, G., and Levine, S. Conservative q-learning for offline reinforcement learning. In Advances in Neural Information Processing Systems, volume 33, pp. 1179–1191, 2020.
- Kushner, H. J. A new method of locating the maximum point of an arbitrary multipeak curve in the presence of noise. Journal of Basic Engineering, 86(1):97–106, 1964.
- Laghuvarapu, S., Lin, Z., and Sun, J. Codrug: Conformal drug property prediction with density estimation under covariate shift. In Oh, A., Naumann, T., Globerson, A., Saenko, K., Hardt, M., and Levine, S. (eds.), Advances in Neural Information Processing Systems, volume 36, pp. 37728–37747. Curran Associates, Inc., 2023.
- Langford, J. and Zhang, T. The epoch-greedy algorithm for multi-armed bandits with side information. In Advances in Neural Information Processing Systems, volume 20, 2008.
- Lei, L. and Candès, E. J. Conformal inference of counterfactuals and individual treatment effects. Journal of the Royal Statistical Society Series B: Statistical Methodology, 83(5):911–938, 2021.
- Lekeufack, J., Angelopoulos, A. N., Bajcsy, A., Jordan, M. I., and Malik, J. Conformal decision theory: Safe autonomous decisions from imperfect predictions. In 2024 IEEE International Conference on Robotics and Automation (ICRA), pp. 11668–11675. Ieee, 2024.

- Li, L., Chu, W., Langford, J., and Schapire, R. E. A contextual-bandit approach to personalized news article recommendation. In Proceedings of the 19th International Conference on World Wide Web, pp. 661–670, 2010.
- Lindemann, L., Cleaveland, M., Shim, G., and Pappas, G. J. Safe planning in dynamic environments using conformal prediction. IEEE Robot. Autom. Lett., 8(8):5116–5123, August 2023.
- Lindemann, L., Zhao, Y., Yu, X., Pappas, G. J., and Deshmukh, J. V. Formal verification and control with conformal prediction. arXiv preprint arXiv:2409.00536, 2024.
- Luo, R., Zhao, S., Kuck, J., Ivanovic, B., Savarese, S., Schmerling, E., and Pavone, M. Sample-efficient safety assurances using conformal prediction. Int. J. Rob. Res., 43(9):1409–1424, August 2024.
- Metevier, B., Giguere, S., Brockman, S., Kobren, A., Brun, Y., Brunskill, E., and Thomas, P. S. Offline contextual bandits with high probability fairness guarantees. In Advances in Neural Information Processing Systems, volume 32, 2019.
- Metropolis, N., Rosenbluth, A. W., Rosenbluth, M. N., Teller, A. H., and Teller, E. Equation of state calculations by fast computing machines. The journal of chemical physics, 21(6):1087–1092, 1953.
- Mohri, C. and Hashimoto, T. Language models with conformal factuality guarantees. In Proceedings of the 41st International Conference on Machine Learning, volume 235 of Proceedings of Machine Learning Research, pp. 36029–36047. Pmlr, 2024.
- Nair, Y. and Janson, L. Randomization tests for adaptively collected data. arXiv preprint arXiv:2301.05365, 2023.
- Norman, D. A. The Design of Everyday Things. Basic Books, 1988.
- Overman, W., Vallon, J. J., and Bayati, M. Aligning model properties via conformal risk control. Advances in Neural Information Processing Systems, 37:110702–110722, 2024.
- Papadopoulos, H., Proedrou, K., Vovk, V., and Gammerman, A. Inductive confidence machines for regression. In European conference on machine learning, pp. 345–356. Springer, 2002.
- Pedregosa, F., Varoquaux, G., Gramfort, A., Michel, V., Thirion, B., Grisel, O., Blondel, M., Prettenhofer, P., Weiss, R., Dubourg, V., Vanderplas, J., Passos, A., Cournapeau, D., Brucher, M., Perrot, M., and Duchesnay, E. Scikit-learn: Machine learning in Python. Journal of Machine Learning Research, 12:2825–2830, 2011.
- Prinster, D., Liu, A., and Saria, S. Jaws: Auditing predictive uncertainty under covariate shift. Advances in Neural Information Processing Systems, 35:35907–35920, 2022.
- Prinster, D., Saria, S., and Liu, A. Jaws-x: addressing efficiency bottlenecks of conformal prediction under standard and feedback covariate shift. In International Conference on Machine Learning, pp. 28167–28190. Pmlr, 2023.
- Prinster, D., Stanton, S., Liu, A., and Saria, S. Conformal validity guarantees exist for any data distribution (and how to find them). Icml, 2024.
- Prinster, D., Han, X., Liu, A., and Saria, S. Watch: Adaptive monitoring for ai deployments via weighted-conformal martingales. International Conference on Machine Learning, 2025.
- Quach, V., Fisch, A., Schuster, T., Yala, A., Sohn, J. H., Jaakkola, T. S., and Barzilay, R. Conformal language modeling. International Conference on Learning Representations, 2024.
- Rafailov, R., Sharma, A., Mitchell, E., Ermon, S., Manning, C. D., and Finn, C. Direct preference optimization: Your language model is secretly a reward model. In Advances in Neural Information Processing Systems, volume 36, pp. 53728–53741, 2023.
- Raiffa, H. and Schlaifer, R. Applied statistical decision theory. MIT Press, 1961.
- Rajpurkar, P., Zhang, J., Lopyrev, K., and Liang, P. SQuAD: 100,000+ questions for machine comprehension of text. In Proceedings of the 2016 Conference on Empirical Methods in Natural Language Processing, pp. 2383–2392, 2016.
- Rhodes, B., Xu, K., and Gutmann, M. U. Telescoping density-ratio estimation. In Larochele, H., Ranzato, M., Hadsell, R., Balcan, M., and Lin, H. (eds.), Advances in Neural Information Processing Systems, volume 33, pp. 4905–4916, 2020.
- Schulman, J., Levine, S., Abbeel, P., Jordan, M., and Moritz, P. Trust region policy optimization. In International conference on machine learning, pp. 1889–1897. Pmlr, 2015.
- Schulman, J., Wolski, F., Dhariwal, P., Radford, A., and Klimov, O. Proximal policy optimization algorithms. arXiv preprint arXiv:1707.06347, 2017.
- Shalev-Shwartz, S., Shamir, O., Srebro, N., and Sridharan, K. Learnability, stability and uniform convergence. The Journal of Machine Learning Research, 11:2635–2670, 2010.

- Singh, S., Sarna, N., Li, Y., Li, Y., Orfanoudaki, A., and Berger, M. Distribution-free risk assessment of regression-based machine learning algorithms. arXiv preprint arXiv:2310.03545, 2023.
- Smith, J. E. and Winkler, R. L. The optimizer’s curse: Skepticism and postdecision surprise in decision analysis. Management Science, 52(3):311–322, 2006.
- Snell, J. C. and Griffiths, T. L. Conformal prediction as bayesian quadrature. International Conference on Machine Learning, 2025.
- Stanton, S., Maddox, W., and Wilson, A. G. Bayesian optimization with conformal prediction sets. In International Conference on Artificial Intelligence and Statistics, pp. 959–986. Pmlr, 2023.
- Straitouri, E., Wang, L., Okati, N., and Rodriguez, M. G. Improving expert predictions with conformal prediction. In International Conference on Machine Learning, pp. 32633–32653. Pmlr, 2023.
- Stutz, D., Cemgil, A. T., Doucet, A., et al. Learning optimal conformal classifiers. International Conference on Learning Representations, 2022.
- Sugiyama, M., Suzuki, T., and Kanamori, T. Density Ratio Estimation in Machine Learning. Cambridge University Press, 2012.
- Sui, Y., Gotovos, A., Burdick, J., and Krause, A. Safe exploration for optimization with gaussian processes. In International Conference on Machine Learning, pp. 997–1005. Pmlr, 2015.
- Sun, J., Jiang, Y., Qiu, J., Nobel, P., Kochenderfer, M. J., and Schwager, M. Conformal prediction for uncertainty-aware planning with diffusion dynamics model. In Oh, A., Naumann, T., Globerson, A., Saenko, K., Hardt, M., and Levine, S. (eds.), Advances in Neural Information Processing Systems, volume 36, pp. 80324–80337. Curran Associates, Inc., 2023.
- Taufiq, M. F., Ton, J.-F., Cornish, R., Teh, Y. W., and Doucet, A. Conformal off-policy prediction in contextual bandits. Advances in Neural Information Processing Systems, 35: 31512–31524, 2022.
- Teneggi, J., Tivnan, M., Stayman, W., and Sulam, J. How to trust your diffusion model: A convex optimization approach to conformal risk control. In International Conference on Machine Learning, pp. 33940–33960. Pmlr, 2023.
- Theodorou, E., Buchli, J., and Schaal, S. A generalized path integral control approach to reinforcement learning. The Journal of Machine Learning Research, 11:3137–3181, 2010.
- Thomas, P., Theodorou, G., and Ghavamzadeh, M. High confidence policy improvement. In Proceedings of the 32nd International Conference on Machine Learning, volume 37 of Proceedings of Machine Learning Research, pp. 2380–2388. Pmlr, 2015.
- Thomas, P. S., Castro da Silva, B., Barto, A. G., Giguere, S., Brun, Y., and Brunskill, E. Preventing undesirable behavior of intelligent machines. Science, 366(6468): 999–1004, 2019.
- Tibshirani, R. J., Foygel Barber, R., Candes, E., and Ramdas, A. Conformal prediction under covariate shift. Advances in neural information processing systems, 32, 2019.
- Tierney, L. Markov chains for exploring posterior distributions. the Annals of Statistics, pp. 1701–1728, 1994.
- Todorov, E. Efficient computation of optimal actions. Proceedings of the national academy of sciences, 106 (28):11478–11483, 2009.
- Trabucco, B., Kumar, A., Geng, X., and Levine, S. Conservative objective models for effective offline model-based optimization. In Advances in Neural Information Processing Systems, volume 34, pp. 20089–20102, 2021.
- Uehara, M., Zhao, Y., Black, K., Hajiramezani, E., Scalia, G., Diamant, N. L., Tseng, A. M., Biancalani, T., and Levine, S. Fine-tuning of continuous-time diffusion models as entropy-regularized control. arXiv preprint arXiv:2402.15194, 2024.
- University of Toronto. The DELVE manual: Data for evaluating learning in valid experiments. <https://www.cs.toronto.edu/~delve/data/kin/desc.html>, 1996.
- Von Neumann, J. et al. Various techniques used in connection with random digits. John von Neumann, Collected Works, 5:768–770, 1963.
- Vovk, V. and Bendtsen, C. Conformal predictive decision making. In Conformal and Probabilistic Prediction and Applications, pp. 52–62. Pmlr, 2018.
- Vovk, V., Gammerman, A., and Shafer, G. Algorithmic learning in a random world. Springer, 2005.
- Vovk, V., Shen, J., Manokhin, V., and Xie, M.-g. Nonparametric predictive distributions based on conformal prediction. In Conformal and probabilistic prediction and applications, pp. 82–102. Pmlr, 2017.
- Wang, H. and Ning, C. Conformal prediction in the loop: A feedback-based uncertainty model for trajectory optimization. In Advances in Neural Information Processing Systems, volume 39, 2025.

- Watkins, C. J. and Dayan, P. Q-learning. Machine Learning, 8(3-4):279–292, 1992.
- Wei, J., Bosma, M., Zhao, V., Guu, K., Yu, A. W., Lester, B., Du, N., Dai, A. M., and Le, Q. V. Finetuned language models are zero-shot learners. In International Conference on Learning Representations, 2022.
- Williams, R. J. Simple statistical gradient-following algorithms for connectionist reinforcement learning. Machine Learning, 8:229–256, 1992.
- Yang, Y., Kuchibhotla, A. K., and Tchetgen Tchetgen, E. Doubly robust calibration of prediction sets under covariate shift. Journal of the Royal Statistical Society Series B: Statistical Methodology, 86(4):943–965, 2024.
- Yeh, C., Christianson, N., Wu, A., Wierman, A., and Yue, Y. End-to-end conformal calibration for optimization under uncertainty. Transactions on Machine Learning Research, 2024.
- Yeh, C., Christianson, N., Wierman, A., and Yue, Y. Conformal risk training: End-to-end optimization of conformal risk control. arXiv preprint arXiv:2510.08748, 2025.
- Zaffran, M., Féron, O., Goude, Y., Josse, J., and Dieuleveut, A. Adaptive conformal predictions for time series. In International conference on machine learning, pp. 25834–25866. Pmlr, 2022.
- Zhang, D., Chatzimparmpas, A., Kamali, N., and Hullman, J. Evaluating the utility of conformal prediction sets for ai-advised image labeling. In Proceedings of the 2024 CHI Conference on Human Factors in Computing Systems, pp. 1–19, 2024a.
- Zhang, Y., Shi, C., and Luo, S. Conformal off-policy prediction. In International Conference on Artificial Intelligence and Statistics, pp. 2751–2768. Pmlr, 2023.
- Zhang, Y., Park, S., and Simeone, O. Bayesian optimization with formal safety guarantees via online conformal prediction. IEEE Journal of Selected Topics in Signal Processing, 19(1):45–59, 2024b.
- Zhao, M., Simmons, R., Admoni, H., Ramdas, A., and Bajcsy, A. Conformalized interactive imitation learning: Handling expert shift and intermittent feedback. arXiv preprint arXiv:2410.08852, 2024.
- Zhou, W., Orfanoudaki, A., and Zhu, S. Conformalized decision risk assessment. arXiv preprint arXiv:2505.13243, 2025.

Supplementary Material

Table of Contents

A	Extended Related Work	16
B	Proofs	20
C	Implementation Details	34
D	Medical QA Experiments	39
E	Tabular Active Learning Experiments	43
F	Sequence Optimization Experiments	45

A. Extended Related Work

A.1. Conservative Model-Based Optimization

The tension between optimization performance and reliability has deep roots in decision theory, from early work on optimal decision-making under uncertainty (Raiffa & Schlaifer, 1961) to stochastic methods for optimization under noise (Kushner, 1964). The *optimizer’s curse* (Smith & Winkler, 2006) captures the key challenge: when decisions are selected by maximizing an estimated value function, the selected action is systematically biased toward outcomes whose value is overestimated. Crucially, this bias persists even when the value estimates are unbiased on average and arises from the act of selection itself. Among many uncertain alternatives, those with the largest positive estimation errors are most likely to be chosen. In the context of sequential decision making and policy optimization, this effect manifests when an optimized policy is trained to maximize expected reward under limited or noisy feedback, leading it to concentrate probability mass on actions whose apparent advantage is driven by estimation error rather than true performance. As a result, policies that appear optimal in expectation may perform poorly when deployed, particularly when they extrapolate beyond regions where reliable evidence is available. In sequential settings, this effect compounds. Aggressive optimization shifts the data distribution away from regions where the estimators are reliable, further degrading the estimates and creating more error for the optimizer to exploit.

Various communities have aimed at guiding models toward high-performing solutions while explicitly constraining distribution shift away from trusted data or policies. In stochastic control and reinforcement learning, entropy-regularized control and KL-penalized objectives constrain optimized policies to stay close to a reference distribution (Todorov, 2009; Fox et al., 2016). Related formulations arise in path integral control and KL-regularized path measures (Kappen, 2005; Theodorou et al., 2010). Trust-region policy optimization methods can be viewed as a practical instantiation that explicitly bound policy updates with local constraints (Schulman et al., 2015; 2017). In offline and batch reinforcement learning, conservative objectives penalize actions whose value estimates rely on out-of-distribution extrapolation (Kumar et al., 2020; Trabucco et al., 2021). More recently, the control-theoretic perspective has been extended to generative model fine-tuning. Fine-tuning diffusion and flow models to maximize the expected reward while retaining the pretrained model information via KL regularization has been framed as an entropy-regularized optimal control problem (Uehara et al., 2024; Domingo-Enrich et al., 2025), and generalized to other utilities and divergence measures (De Santi et al., 2025).

Finally, in black-box optimization, trust-region Bayesian optimization restricts search to local regions where surrogate models are reliable (Eriksson et al., 2019), while safe Bayesian optimization enforces hard safety constraints to prevent evaluation in unsafe regions (Sui et al., 2015; Berkenkamp et al., 2016; Kirschner et al., 2019; Berkenkamp et al., 2023). All of these methods operationalize safety by bounding how far the optimized distribution may deviate from a known baseline.

In practice, however, the strength of this constraint is governed by a scalar hyperparameter that has no intrinsic semantic interpretation. Whether expressed as a KL penalty weight, a likelihood ratio threshold, or a trust-region radius, this parameter controls the degree of aggressiveness in optimization but does not directly correspond to any declarative risk criterion, such as a target failure rate. As a result, practical deployment requires solving a secondary *hyperparameter selection problem*: one must select many candidate values of the constraint parameter and empirically evaluate their downstream risk in order to

Table 1. Summary comparison of selected related work on conformal prediction for decision making under agent-induced shifts.

Method Group References	1. Agent-Induced Data Shift	2. Action Space	3. Type of Risk Control		
			Prediction Set Miscoverage $\mathbb{1}\{Y_t \notin \hat{C}_\alpha(X_t)\}$	λ -Parameterized Losses $L_t(A_t(\lambda))$	Unparameterizable Losses (β -Param. Policy) $L_t(A_t), A_t \sim p_t(\beta)$
Conformal Prediction Vovk et al. (2005) Vovk & Bendtsen (2018)	✗	Small/ Finite	✓	✗	✗
Weighted Conformal Pred. Tibshirani et al. (2019) Fannjiang et al. (2022) Stanton et al. (2023) Nair & Janson (2023) Prinster et al. (2024)	Single-Round	Small/ Finite	✓	✗	✗
	Multi-Round	Contin. Small/ Finite	✓	✗	✗
Conformal Risk Control Angelopoulos et al. (2024) Lekeufack et al. (2024)	Single-Round	Small/ Finite	✓	✓	✗
	Eventually safe		✓	✓	✗
Conformal Policy Control (Proposed)	Multi-Round	Large/ ∞	✓	✓	✓

identify a satisfactory operating point. Critically, this calibration must be performed *on-policy*, since the risk of interest depends on the distribution induced by each specific choice of the hyperparameter. This requirement is costly and introduces further feedback-loop dependencies (Bergstra et al., 2011; Feurer & Hutter, 2019).

Yet the distribution shift these methods seek to control is self-inflicted. The agent chooses its own policy, and therefore knows the likelihood ratio between any candidate policy and the safe baseline in closed form. The distribution shift is not an external unknown but a consequence of the agent’s own design. This means the hyperparameter selection problem can be solved with off-policy data from the safe policy alone, provided the calibration is done carefully. Conformal techniques provide exactly this kind of careful calibration.

A.2. Conformal Methods

Conformal prediction under distribution shift in high-dimensional spaces

Conformal prediction, originally developed for exchangeable or i.i.d. data by (Vovk et al., 2005), has been extended to a variety of distribution shift settings. Closest to the current paper are *weighted* conformal methods that *proactively adapt* to distribution shift by re-weighting calibration data using knowledge of the change, though another line of work develops conformal-inspired methods for *retroactively reacting* to adversarial shifts over time (e.g., Gibbs & Candès (2021); Zaffran et al. (2022); Bastani et al. (2022); Angelopoulos et al. (2023)). Among weighted conformal methods, those most relevant to the present work are methods tailored for covariate shift (Tibshirani et al., 2019; Prinster et al., 2022; Yang et al., 2024; Jonkers et al., 2024), and especially its extensions in which the training and test data are dependent, such as one-step (Fannjiang et al., 2022; Prinster et al., 2023) and multi-step (Nair & Janson, 2023; Prinster et al., 2024) feedback covariate shift, as is the case in the policy optimization setting. Also relevant are the fixed-weight methods of Barber et al. (2023), which bound the coverage violation due to misspecified data-independent weights, and the unifying weighted conformal framework of Barber & Tibshirani (2025).

When deviating from the assumption of exchangeable calibration and test data, any analysis of proactive conformal prediction methods invokes quantities characterizing the relationship between the calibration and test distributions, such as their density ratios or divergences. Therefore, despite the advances in theory, deployment of conformal prediction methods in practice in distribution shift settings has been hamstrung by the practical difficulty of evaluating such quantities, particularly in high-dimensional spaces. Consider the combinatorially large action spaces involved in high-impact applications such as biological sequence design. Unless modeling the distribution using factorizations amenable to tractable computation (e.g., autoregressive generative models), it is generally computationally intractable to evaluate the density of distributions over sequence space, as exact computation of normalizing constants is infeasible. As a workaround, some approaches have resorted to density ratio estimation (Stanton et al., 2023; Laghuvarapu et al., 2023; Fannjiang & Park, 2025; Correia & Louzos, 2025), a task that is also challenging and ill-posed in high dimensions (Rhodes et al., 2020), and which nullifies

validity guarantees due to estimation error. In the present work, we circumvent the difficulty of evaluating density ratios between the calibration and test policies by making their density ratio itself the tunable control parameter, as follows. We first assume existence of an initial safe policy, π_0 , that satisfies the safety constraint, as well as naively optimized policies at each time, π_t . At each time, we define a family of “constrained policies” that interpolates between π_0 and π_t by clipping their density ratio, $\pi_t(\cdot)/\pi_0(\cdot)$, at an upper bound, β_t (Eq. (5)). By making this density ratio upper bound, β_t , the tunable control parameter, we have done away with the need to estimate the density ratio altogether.

Conformal methods for decision-making in the offline setting

Conformal methods, by which we mean conformal prediction techniques and their generalizations to settings beyond constructing instance-wise prediction sets with coverage guarantees, have also been developed for various decision-making settings. Vovk & Bendtsen (2018) laid the groundwork for conformal decision-making, demonstrating how conformal prediction (specifically conformal predictive distributions (Vovk et al., 2017)) can be used to make decisions that satisfy a notion of efficiency. They noted, however, that they had “limited [themselves] to analyzing a given batch of data, without attempting active learning, and this limitation has made it possible to develop a fairly systematic theory.”

Indeed, following Vovk & Bendtsen (2018), subsequent work on conformal methods for decision making has largely also assumed an offline (i.e., non-active) setting, where training and calibration are entirely independent of test-time decisions: that is, where pre-deployment training and calibration cannot influence distributions at test time, and vice versa (without breaking statistical guarantees). For instance, see Hullman et al. (2025) for a recent overview. Approaches in this offline setting have included conformal prediction sets for individual treatment effect estimates (Lei & Candès, 2021), off-policy prediction (Taufiq et al., 2022; Zhang et al., 2023), extending conformal prediction sets to handle notions of risk beyond miscoverage (Bates et al., 2021; Angelopoulos et al., 2024), risk assessment (Prinster et al., 2022; Singh et al., 2023; Zhou et al., 2025), developing connections with Bayesian decision theory (Hoff, 2023; Snell & Griffiths, 2025), and designing conformal sets for (or the filtering of) outputs of fixed/pre-trained generative models (Quach et al., 2024; Teneggi et al., 2023; Mohri & Hashimoto, 2024; Cherian et al., 2024; Overman et al., 2024; Jiang et al., 2025). Another line of work has developed conformal-inspired optimization procedures to simulate decision making during training (Colombo & Vovk, 2020; Stutz et al., 2022; Cortes-Gomez et al., 2025; Yeh et al., 2024; 2025), but notably, these methods all require a further split of the data beyond that of split conformal (Papadopoulos et al., 2002), thus effectively side-stepping the “optimizer’s curse” at the cost of reduced data efficiency.⁵

While Kiyani et al. (2025) theoretically demonstrated that prediction sets are particularly suitable for risk-averse decision-making and several works have empirically demonstrated the utility of prediction sets for human decision makers (Straitouri et al., 2023; Cresswell et al., 2024; Zhang et al., 2024a), there nonetheless remains a gap between methodological progress and practical impact of conformal methods (Hullman et al., 2025). Arguably, this persistent gap is due to the fact that predictions (and consequently, prediction sets) are almost never the end goal in practice. Instead, the end goal in practice is often to control how prediction error affects the specific downstream decisions, or the policy, of interest.

Conformal methods for decision-making in the active setting

In the active setting, where an agent’s actions may influence the observed data distribution, there are two main threads of literature that parallel corresponding methods for conformal prediction under distribution shift. The first thread uses ideas from weighted conformal to proactively adapt prediction sets to agent-induced shifts: Fannjiang et al. (2022) extended the weighted conformal methods of Tibshirani et al. (2019) to a one-step instance of “feedback covariate shift,” where the input distribution of a single test batch can depend on the training data. Inspired by this work, Stanton et al. (2023) incorporated weighted conformal methods into Bayesian optimization, aiming to close the decision-making loop by allowing conformal calibration and optimization to bidirectionally influence each other; however, they noted gaps in the theory that prevented the desired guarantees from being realized. Prinster et al. (2023) extended Fannjiang et al. (2022)’s methods to cross-validation-style conformal calibration; Nair & Janson (2023) introduced an extension to multiple rounds of dependent covariate shifts; and Prinster et al. (2024) extended weighted conformal methods to any data distribution, with multiround agent-induced covariate shifts as a main focus. However, these prior works differ from the present paper in several ways: they all operate *descriptively* to adapt prediction sets for a fixed policy, whereas our methods function *prescriptively*, using conformal calibration to *find* a risk-controlling policy; in combinatorial action spaces, they are bottlenecked by challenges of

⁵That is, these “conformal training” works typically require at least three disjoint splits of the data to maintain statistical validity: a “proper” training set for learning, a validation set used for hyperparameter tuning (or simulating conformal calibration), and a separate fresh calibration set at test time for inference. In contrast, the present paper’s conformal policy control methods avoid such an additional data split by carefully reweighting the calibration data to adjust for data-dependent policy selection.

density-ratio estimation and normalization; and they focus on (mis)coverage rather than more general notions of risk.

The second line of conformal methods in the active setting uses ideas from online adversarial conformal (e.g., Gibbs & Candès (2021)) to retroactively learn decision rules over time: Feldman et al. (2023) extended the online algorithm of Gibbs & Candès (2021) to more general loss functions (similarly as Bates et al. (2021); Angelopoulos et al. (2024) did in the offline setting), and Lekeufack et al. (2024) extended those ideas to a conformal decision theory framework, where the online learning update directly steers an agent’s decisions at the next timestep. Zhang et al. (2024b) use ideas from online adversarial conformal for Bayesian optimization and Zhao et al. (2024) for imitation learning. These works achieve bounds on the long-term average risk as the number of time steps grows indefinitely. In robotics, conformal prediction has also been used to construct predictive sets of trajectories, which are used to make planning or control procedures safer (Lindemann et al., 2023; Luo et al., 2024; Sun et al., 2023; Wang & Ning, 2025; Lindemann et al., 2024).

Conformal selection and high-probability risk control

Along a different vein, motivated by candidate selection problems that arise in drug discovery, conformal selection methods (Jin & Candès, 2022; 2025; Bai & Jin, 2024; Gui et al., 2025) merge ideas from conformal prediction and multiple testing to select designs from a pool of individual candidates, such that the false discovery rate, or expected proportion of selected designs whose label does not surpass a desired threshold, is controlled. While these methods assume access to a pool of exchangeable (e.g., i.i.d.) candidates, in some applications—for example, biological sequence design—this is not a natural setting. Instead, it is more relevant to reason about generating candidates from some distribution, which brings us to our problem of how to select a generative model that controls risk as desired. Fannjiang & Park (2025) tackle this problem as a multiple testing problem to arrive at high-probability guarantees of risk control. Such high-probability risk control guarantees are akin in spirit to prior works on risk controlling prediction sets (Bates et al., 2021) and the Learn-then-Test framework (Angelopoulos et al., 2025), which provide high-probability guarantees for monotonic and non-monotonic losses respectively. In contrast, we build on techniques from conformal risk control (Angelopoulos et al., 2024) to achieve guarantees in expectation, which typically provides tighter risk control. Relative to conformal risk control, we also introduce and focus on the policy control setting, wherein the control parameter directly controls the agent’s policy, to fully connect the decision-making loop, circumvent challenges of density-ratio estimation, and address the optimizer’s curse head-on.

A.3. Seldonian Algorithms

Seldonian algorithms (Thomas et al., 2019) provide a framework for constructing machine learning systems that satisfy user-specified behavioral constraints with high probability. The approach builds on earlier work on high-confidence policy improvement (Thomas et al., 2015), which introduced the use of concentration inequalities to obtain probabilistic guarantees on policy performance. Rather than requiring users to tune abstract regularization weights or penalty coefficients, Seldonian algorithms allow direct specification of constraints such as “the probability of causing harm should be at most 5%.” The framework uses concentration inequalities to derive high-probability bounds on constraint satisfaction, returning a solution only when sufficient evidence exists that the constraints will be met.

The Seldonian framework has been extended in several directions. Metevier et al. (2019) adapted the approach to contextual bandits with fairness constraints, demonstrating how user-specified fairness definitions can be enforced with high-probability guarantees. Chandak et al. (2020) addressed non-stationary MDPs by incorporating time-series forecasting to anticipate distribution shift. Giguere et al. (2022) extended the framework to handle demographic shift between training and deployment, providing guarantees that remain valid when the population composition changes.

Both Seldonian algorithms and conformal policy control share the goal of translating user-specified risk tolerances directly into algorithmic constraints, eliminating the need for trial-and-error hyperparameter tuning. However, the two frameworks differ in the nature of their guarantees and the distinction between *certification* and *regulation*. Seldonian algorithms provide *conditional, high-probability* bounds: with probability at least $1 - \delta$, the deployed policy satisfies the specified constraints. In contrast, conformal methods provide *marginal, expected value* guarantees: on average, the expected loss under the deployed policy is bounded by the user-specified level α . Neither guarantee type strictly dominates the other. High-probability bounds are more conservative but offer protection against worst-case outcomes. Expected value bounds are tighter on average but permit occasional constraint violations. The greatest difference between our work and Seldonian algorithms is our method can be used to safely deploy (control the expected risk of) a model that would not be safe otherwise through the rejection sampling regulation procedure. By contrast, a Seldonian algorithm can certify that the solution it returns satisfies its constraints with high probability, however it cannot regulate an existing solution trained by some third-party algorithm.

B. Proofs

B.1. Proof generalized conformal risk control with exchangeable data.

Notation:

- **Data (sequences of random variables and observed values):** For all $i \in \mathbb{N}$, denote the random variable for the i -th data sample as $Z_i := (X_i, Y_i) \in \mathcal{X} \times \mathcal{Y} = \mathcal{Z}$, and denote observed value of that random variable in lower case as $z_i := (x_i, y_i) \in \mathcal{X} \times \mathcal{Y} = \mathcal{Z}$. Similarly, denote a sequence of random variables as $Z_{1:m} := (Z_1, \dots, Z_m)$ and a sequence of observed data values as $z_{1:m} := (z_1, \dots, z_m)$ for any $m \in \mathbb{N}$. To concisely denote indices, let $[m] := \{1, \dots, m\}$.
- **Hyperparameter space:** Let $\Lambda \subseteq \mathbb{R}$ be the space of hyperparameters. So, $\lambda \in \Lambda$ denotes a particular hyperparameter in this space.
- **Loss functions:** For some real-valued function $g : \mathcal{Z} \times \Lambda \rightarrow \mathbb{R}$, and for all $\lambda \in \Lambda$ and all $i \in \mathbb{N}$, let $L_i(\lambda) := g(Z_i, \lambda)$ denote the loss function determined by a random variable Z_i and parameter $\lambda \in \Lambda$, and let $\ell_i(\lambda) := g(z_i, \lambda)$ denote the loss function determined by the observed value z_i and parameter $\lambda \in \Lambda$. To emphasize when no particular λ has yet been given as an argument, we will use $L_i(\cdot) := g(Z_i, \cdot)$ to denote the loss function with randomness over Z_i not yet determined, and we will use $\ell_i(\cdot) := g(z_i, \cdot)$ to denote the loss function for observed value z_i .
- **Bags:** For any sequence $v_{1:m} := (v_1, \dots, v_m)$, let $\wr v_{1:m} \wr$ denote the *bag* (or multiset) containing the values of that sequence $v_{1:m}$ (but importantly, $\wr v_{1:m} \wr$ does *not* contain the information about the order of $v_{1:m}$). For example, $\wr (1, 7, 42, 7) \wr$ conveys that there is one 1, two 7s, and one 42 in the bag, but it does *not* convey the order that these appeared in the sequence $(1, 7, 42, 7)$. In particular, with this notation, for the random variables $Z_{1:m}$, let $\wr Z_{1:m} \wr$ denote the bag containing those random variables; for observed values $z_{1:m}$, let $\wr z_{1:m} \wr$ denote the bag containing those observed values; and thus $\wr Z_{1:m} \wr = \wr z_{1:m} \wr$ denotes the event of observing $\wr z_{1:m} \wr$, in other words, that each Z_i takes a different value in $\wr z_{1:m} \wr$, but it is not yet known *which* value (for all $i \in [m]$).
- **Distributions:** Let $F_{Z_{1:m}} := F_{Z_1, \dots, Z_m}$ denote the joint distribution function for Z_1, \dots, Z_m , and let $F_{\wr Z_{1:m} \wr} := F_{\wr z_{1:m} \wr}$ denote the (pushforward) distribution induced by the mapping $(z_1, \dots, z_m) \rightarrow \wr z_{1:m} \wr$.

Theorem B.1 (Restatement of Theorem 4.2). *Assume exchangeable $L_i(\lambda)$. Define $\lambda_{\max} := \sup \Lambda \in \Lambda$ and assume*

$$L_i(\lambda_{\max}) \leq \alpha, \quad \sup_{\lambda} L_i(\lambda) \leq B < \infty \quad \text{almost surely.}$$

If the $L_i(\lambda)$ are K -Lipschitz in λ and $\hat{\lambda}_+$ is ϵ -replace-one stable, then

$$\mathbb{E}[L_{n+1}(\hat{\lambda}_+)] \leq \alpha + K\epsilon.$$

Proof.

Step 0: Law of total expectation over draw of bag.

Expanding $\mathbb{E}[L_{n+1}(\hat{\lambda}_+)]$ via the law of total expectation over the event $\wr Z_{1:n+1} \wr = \wr z_{1:n+1} \wr$, we have

$$\mathbb{E}[L_{n+1}(\hat{\lambda}_+)] = \mathbb{E}_{F_{\wr Z_{1:n+1} \wr}} \left[\mathbb{E} \left[L_{n+1}(\hat{\lambda}_+) \mid \wr Z_{1:n+1} \wr = \wr z_{1:n+1} \wr \right] \right]. \quad (7)$$

We can thus see that, to prove the desired result, it is sufficient to upper bound $\mathbb{E}[L_{n+1}(\hat{\lambda}_+) \mid \wr Z_{1:n+1} \wr = \wr z_{1:n+1} \wr]$ almost surely given any draw of the bag, $\wr Z_{1:n+1} \wr \sim F_{\wr Z_{1:n+1} \wr}$.

Step 1: Deterministic inequalities on bag-conditional risks.

Define the following family of thresholds:

$$\hat{\lambda}_+(\wr L_{1:m} \wr, \gamma) = \inf \left\{ \lambda_0 \in \Lambda \quad : \quad \forall \quad \text{fixed } \lambda \geq \lambda_0, \quad \sum_{i=1}^m \frac{l_i(\lambda)}{m} \leq \gamma \right\}.$$

When the set is empty, define $\hat{\lambda}_+(\{L_{1:m}\}, \gamma) = \lambda_{\max}$.

By the right-continuity of $L_i(\cdot)$ (for all $i \in \mathbb{N}$), the sum $\sum_{i=1}^m \frac{L_m(\lambda)}{m}$ is right-continuous for any $Z_{1:m}$, which gives us the following deterministic inequality for any γ :

$$\sum_{i=1}^m \frac{L_i(\lambda)}{m} \leq \gamma \quad \forall \quad \text{fixed } \lambda \geq \hat{\lambda}_+(\{L_{1:m}\}; \gamma). \quad (8)$$

Step 2: Showing an oracle procedure deterministically controls the bag-conditional risk.

Using the family of thresholds we defined above and applying it to the bag of loss functions for both the calibration set and the test point, define the oracle threshold as

$$\lambda_+^* := \hat{\lambda}_+(\{L_{1:n+1}\}, \alpha). \quad (9)$$

Now, consider the quantity $\mathbb{E}[L_{n+1}(\lambda_+^*) \mid \{Z_{1:n+1}\} = \{z_{1:n+1}\}]$, which we can view as the bag-conditional oracle risk. That is, we can interpret this quantity as the expected value that the random variable $L_{n+1}(\lambda_+^*)$ will take on, given the bag of data $\{z_{1:n+1}\}$. Note that conditioning on the bag of data, $\{z_{1:n+1}\}$, implies the event of observing the bag of loss functions, $\{l_{1:n+1}\}$,⁶ which thereby determines the value of λ_+^* , since λ_+^* is a symmetric function of $\{z_{1:n+1}\}$.

This fact, that λ_+^* is a symmetric function of (and thus determined by) the bag of data, implies that $L_{n+1}(\lambda_+^*)$ will take a value in $\{l_1(\lambda_+^*), \dots, l_{n+1}(\lambda_+^*)\}$ and the specific value $L_{n+1}(\lambda_+^*)$ will take on is determined by the draw of Z_{n+1} from $\{z_{1:n+1}\}$; that is, given $\{z_{1:n+1}\}$, we have the equivalency $L_{n+1}(\lambda_+^*) = l_i(\lambda_+^*) \iff Z_{n+1} = z_i$ due to $g(\cdot, \lambda_+^*)$ inducing a bijection from $\{z_1, \dots, z_{n+1}\}$ to the bag of loss values $\{l_1(\lambda_+^*), \dots, l_{n+1}(\lambda_+^*)\}$.

First using this observation and the definition of conditional expectation, and secondly using the definition of conditional probability, we have

$$\begin{aligned} \mathbb{E}[L_{n+1}(\lambda_+^*) \mid \{Z_{1:n+1}\} = \{z_{1:n+1}\}] &= \sum_{i=1}^{n+1} l_i(\lambda_+^*) \cdot \mathbb{P}(Z_{n+1} = z_i \mid \{Z_{1:n+1}\} = \{z_{1:n+1}\}) \\ &= \sum_{i=1}^{n+1} l_i(\lambda_+^*) \cdot \frac{\mathbb{P}(Z_{n+1} = z_i, \{Z_{1:n+1}\} = \{z_{1:n+1}\})}{\mathbb{P}(\{Z_{1:n+1}\} = \{z_{1:n+1}\})}. \end{aligned}$$

Applying the law of total probability over permutations ($\sigma : [n+1] \rightarrow [n+1]$) to the probabilities in the numerator and denominator of the RHS, and then simplifying using exchangeability, we have

$$\begin{aligned} \mathbb{E}[L_{n+1}(\lambda_+^*) \mid \{Z_{1:n+1}\} = \{z_{1:n+1}\}] &= \sum_{i=1}^{n+1} l_i(\lambda_+^*) \cdot \frac{\sum_{\sigma: \sigma(n+1)=i} f(z_{\sigma(1)}, \dots, z_{\sigma(n+1)})}{\sum_{\sigma} f(z_{\sigma(1)}, \dots, z_{\sigma(n+1)})} \\ &= \sum_{i=1}^{n+1} l_i(\lambda_+^*) \cdot \frac{\sum_{\sigma: \sigma(n+1)=i} f(z_1, \dots, z_{n+1})}{\sum_{\sigma} f(z_1, \dots, z_{n+1})} \\ &= \sum_{i=1}^{n+1} l_i(\lambda_+^*) \cdot \frac{n!}{(n+1)!} \\ &= \sum_{i=1}^{n+1} \frac{l_i(\lambda_+^*)}{n+1} \end{aligned}$$

⁶That is, implies the event $\{L_1(\cdot), \dots, L_{n+1}(\cdot)\} = \{l_1(\cdot), \dots, l_{n+1}(\cdot)\}$, because the loss functions are defined as $l_i(\cdot) := g(z_i, \cdot)$ for all $i \in \mathbb{N}$.

Now, using Eq. (8),

$$\sum_{i=1}^{n+1} \frac{l_i(\lambda)}{n+1} \leq \alpha \quad \forall \quad \text{fixed } \lambda \geq \lambda_+^*, \quad (10)$$

where here by ‘‘fixed’’ we mean that λ is constant conditional on the bag of data, $\{Z_{1:n+1}\} = \{z_{1:n+1}\}$.

Step 3: Relating the empirically-selected hyperparameter to the oracle parameter

In Step 2, we have shown that an oracle procedure deterministically controls the risk, conditional on the event $\{Z_{1:n+1}\} = \{z_{1:n+1}\}$. However, this oracle procedure cannot be implemented in practice due to requiring knowledge of the test point loss, L_{n+1} ; that is, recall we defined $\lambda_+^* := \hat{\lambda}_+(\{L_{1:n+1}\}, \alpha)$. In this last step of the proof we would now like to prove a deterministic relationship between the oracle parameter, λ_+^* , and the empirically-selected parameter, $\hat{\lambda}_+ := \hat{\lambda}_+(\{L_{1:n}, B\}, \alpha)$, to conclude valid risk control for the empirical method; that is, we would like to deterministically show $\lambda_+^* \leq \hat{\lambda}_+$.

To begin, recall that in Step 2, conditioning on the event $\{Z_{1:n+1}\} = \{z_{1:n+1}\}$ implied that $\hat{\lambda}_+(\{L_{1:n+1}\}, \alpha) = \hat{\lambda}_+(\{l_{1:n+1}\}, \alpha)$. For the empirical parameter, however, conditioning on $\{Z_{1:n+1}\} = \{z_{1:n+1}\}$ does *not* imply what may seem analogous: that is, it could be that $\hat{\lambda}_+(\{L_{1:n}, B\}, \alpha) \neq \hat{\lambda}_+(\{l_{1:n}, B\}, \alpha)$. This is because the event $\{Z_{1:n+1}\} = \{z_{1:n+1}\}$ only allows us to conclude that the n random variables in $\{L_{1:n}\}$ take n distinct values from the bag of $n+1$ observed losses, $\{l_{1:n+1}\}$, but we do not yet know *which* observed losses. That is, what we *can* conclude is, given $\{Z_{1:n+1}\} = \{z_{1:n+1}\}$, that

$$\{Z_{1:n+1}\} = \{z_{1:n+1}\} \implies \{L_{1:n}\} \in \left\{ \{l_{1:n+1 \setminus i}\} \right\}_{i \in [n+1]},$$

where $\{l_{1:n+1 \setminus i}\} := \{l_{1:n+1}\} \setminus \{l_i\}$. Accordingly, conditioning on the event $\{Z_{1:n+1}\} = \{z_{1:n+1}\}$ implies the following equivalence:

$$\lambda_+^* \leq \hat{\lambda}_+(\{L_{1:n}, B\}, \alpha) \text{ almost surely} \iff \lambda_+^* \leq \hat{\lambda}_+(\{l_{1:n+1 \setminus i}, B\}, \alpha) \quad \forall \quad i \in [n+1]. \quad (11)$$

So, we will focus on proving the latter.

Recall that we have assumed that l is bounded above by B (i.e., $\sup_{\lambda} l_i(\lambda) \leq B < \infty$), for any $\lambda \in \Lambda$, deterministically we have

$$\sum_{j \in [n+1]} \frac{l_j(\lambda)}{n+1} \leq \frac{B}{n+1} + \sum_{j \in [n+1] \setminus i} \frac{l_j(\lambda)}{n+1} \quad \forall \quad i \in [n+1], \quad (12)$$

where the right-hand side of the above inequalities can be interpreted as a conservative risk obtained by replacing $l_i(\lambda)$ with the bound B .

Thus, for any λ , we can use (12) to conclude

$$\frac{B}{n+1} + \sum_{j \in [n+1] \setminus i} \frac{l_j(\lambda)}{n+1} \leq \alpha \implies \sum_{j \in [n+1]} \frac{l_j(\lambda)}{n+1} \leq \alpha \quad \forall \quad i \in [n+1]. \quad (13)$$

So, by (13) and the definition of $\hat{\lambda}_+(\{l_{1:n+1 \setminus i}, B\})$, it must hold that

$$\lambda_+^* \leq \hat{\lambda}_+(\{l_{1:n+1 \setminus i}, B\}) \quad \forall \quad i \in [n+1]. \quad (14)$$

Step 4: Analyzing the bag-conditional risk of the empirical procedure via Lipschitz continuity

Now we turn to plugging the empirical algorithm's hyperparameter into the bag-conditional risk, and then analyzing this risk using Lipschitz continuity and a type of stability called "replace-one" stability. This analysis is necessary because $\hat{\lambda}_+ = \hat{\lambda}_+(\mathcal{Z}_{1:n}, B, \alpha)$ is not constant conditional on $\mathcal{Z}_{1:n+1} = \mathcal{z}_{1:n+1}$, so Eq. (10) would not directly apply.

Begin by expanding this quantity by LOTE over the event $Z_{n+1} = z_i$:

$$\begin{aligned} & \mathbb{E}\left[L_{n+1}(\hat{\lambda}_+) \mid \mathcal{Z}_{1:n+1} = \mathcal{z}_{1:n+1}\right] \\ &= \mathbb{E}\left[\mathbb{E}\left[L_{n+1}(\hat{\lambda}_+) \mid \mathcal{Z}_{1:n+1} = \mathcal{z}_{1:n+1}, Z_{n+1} = z_i \mid \mathcal{Z}_{1:n+1} = \mathcal{z}_{1:n+1}\right]\right] \\ &= \sum_{i=1}^{n+1} \mathbb{E}\left[L_{n+1}(\hat{\lambda}_+) \mid \mathcal{Z}_{1:n+1} = \mathcal{z}_{1:n+1}, Z_{n+1} = z_i\right] \cdot \mathbb{P}(Z_{n+1} = z_i \mid \mathcal{Z}_{1:n+1} = \mathcal{z}_{1:n+1}). \end{aligned} \quad (15)$$

Now, note that we can write the inner expectation as

$$\begin{aligned} \mathbb{E}\left[L_{n+1}(\hat{\lambda}_+) \mid \mathcal{Z}_{1:n+1} = \mathcal{z}_{1:n+1}, Z_{n+1} = z_i\right] &= \mathbb{E}\left[L_{n+1}(\hat{\lambda}_+) \mid \mathcal{Z}_{1:n} = \mathcal{z}_{1:n+1 \setminus i}, Z_{n+1} = z_i\right] \\ &= \mathbb{E}\left[L_{n+1}(\hat{\lambda}_+) \mid \mathcal{L}_{1:n} = \mathcal{l}_{1:n+1 \setminus i}, L_{n+1} = l_i\right]. \end{aligned}$$

And recalling that we defined $\hat{\lambda}_+ := \hat{\lambda}_+(\mathcal{L}_{1:n}, B, \alpha)$, we have

$$\begin{aligned} & \mathbb{E}\left[L_{n+1}(\hat{\lambda}_+) \mid \mathcal{Z}_{1:n+1} = \mathcal{z}_{1:n+1}, Z_{n+1} = z_i\right] \\ &= \mathbb{E}\left[L_{n+1}\left(\hat{\lambda}_+(\mathcal{L}_{1:n}, B, \alpha)\right) \mid \mathcal{L}_{1:n} = \mathcal{l}_{1:n+1 \setminus i}, L_{n+1} = l_i\right] \\ &= \mathbb{E}\left[l_i\left(\hat{\lambda}_+(\mathcal{l}_{1:n+1 \setminus i}, B, \alpha)\right) \mid \mathcal{L}_{1:n} = \mathcal{l}_{1:n+1 \setminus i}, L_{n+1} = l_i\right] \\ &= l_i\left(\hat{\lambda}_+(\mathcal{l}_{1:n+1 \setminus i}, B, \alpha)\right). \end{aligned}$$

So, plugging this into Eq. (15), we have

$$\begin{aligned} & \mathbb{E}\left[L_{n+1}(\hat{\lambda}_+) \mid \mathcal{Z}_{1:n+1} = \mathcal{z}_{1:n+1}\right] \\ &= \sum_{i=1}^{n+1} l_i\left(\hat{\lambda}_+(\mathcal{l}_{1:n+1 \setminus i}, B, \alpha)\right) \cdot \mathbb{P}(Z_{n+1} = z_i \mid \mathcal{Z}_{1:n+1} = \mathcal{z}_{1:n+1}) \\ &= \sum_{i=1}^{n+1} l_i\left(\hat{\lambda}_+(\mathcal{l}_{1:n+1 \setminus i}, B, \alpha)\right) \cdot \frac{\mathbb{P}(Z_{n+1} = z_i, \mathcal{Z}_{1:n+1} = \mathcal{z}_{1:n+1})}{\mathbb{P}(\mathcal{Z}_{1:n+1} = \mathcal{z}_{1:n+1})} \end{aligned}$$

Applying the law of total probability over permutations ($\sigma : [n+1] \rightarrow [n+1]$) to the probabilities in the numerator and denominator of the RHS, and then simplifying using exchangeability, we have

$$\begin{aligned} \mathbb{E}\left[L_{n+1}(\hat{\lambda}_+) \mid \mathcal{Z}_{1:n+1} = \mathcal{z}_{1:n+1}\right] &= \sum_{i=1}^{n+1} l_i\left(\hat{\lambda}_+(\mathcal{l}_{1:n+1 \setminus i}, B, \alpha)\right) \cdot \frac{\sum_{\sigma: \sigma(n+1)=i} f(z_{\sigma(1)}, \dots, z_{\sigma(n+1)})}{\sum_{\sigma} f(z_{\sigma(1)}, \dots, z_{\sigma(n+1)})} \\ &= \sum_{i=1}^{n+1} l_i\left(\hat{\lambda}_+(\mathcal{l}_{1:n+1 \setminus i}, B, \alpha)\right) \cdot \frac{\sum_{\sigma: \sigma(n+1)=i} f(z_1, \dots, z_{n+1})}{\sum_{\sigma} f(z_1, \dots, z_{n+1})} \\ &= \sum_{i=1}^{n+1} l_i\left(\hat{\lambda}_+(\mathcal{l}_{1:n+1 \setminus i}, B, \alpha)\right) \cdot \frac{n!}{(n+1)!} \\ &= \frac{1}{n+1} \sum_{i=1}^{n+1} l_i\left(\hat{\lambda}_+(\mathcal{l}_{1:n+1 \setminus i}, B, \alpha)\right). \end{aligned} \quad (16)$$

Importantly, note that in Eq. (16), which is the true bag-conditional risk of the empirical algorithm, that the value of $\hat{\lambda}_+(\{l_{1:n+1 \setminus i}, B\}, \alpha)$ differs for each loss function, l_i , in the summation, which is why we cannot apply Eq. (10) to bound it directly. Instead, we relate Eq. (16) and Eq. (10) using Lipschitz continuity and the replace-one (in)stability of the algorithm.

For all $i \in [n]$, denote the magnitude of perturbation to the hyperparameter $\hat{\lambda}_+(\{l_{1:n}, B\}, \alpha)$ caused by replacing the loss function l_i with l_{n+1} as

$$\epsilon_i = \left| \hat{\lambda}_+(\{l_{1:n}, B\}, \alpha) - \hat{\lambda}_+(\{l_{1:n+1 \setminus i}, B\}, \alpha) \right|.$$

Then, by K -Lipschitz continuity, we know that for all $i \in [n]$, that

$$\left| l_i(\hat{\lambda}_+(\{l_{1:n}, B\}, \alpha)) - l_i(\hat{\lambda}_+(\{l_{1:n+1 \setminus i}, B\}, \alpha)) \right| \leq K \epsilon_i.$$

Then, note that

$$\sum_{i=1}^{n+1} \frac{l_i(\hat{\lambda}_+(\{l_{1:n+1 \setminus i}, B\}, \alpha))}{n+1} \leq \sum_{i=1}^{n+1} \frac{l_i(\hat{\lambda}_+(\{l_{1:n}, B\}, \alpha)) + K \epsilon_i}{n+1} = \sum_{i=1}^{n+1} \frac{l_i(\hat{\lambda}_+(\{l_{1:n}, B\}, \alpha))}{n+1} + \frac{K}{n+1} \sum_{i=1}^{n+1} \epsilon_i$$

By Eq. (14), we know that $\hat{\lambda}_+(\{l_{1:n}, B\}, \alpha) \geq \lambda_+$, and because this $\hat{\lambda}_+(\{l_{1:n}, B\}, \alpha)$ does not depend on i , we can apply Eq. (10) to bound it above by α , which gives

$$\begin{aligned} \sum_{i=1}^{n+1} \frac{l_i(\hat{\lambda}_+(\{l_{1:n+1 \setminus i}, B\}, \alpha))}{n+1} &\leq \alpha + \frac{K}{n+1} \sum_{i=1}^{n+1} \epsilon_i \\ \iff \mathbb{E}[L_{n+1}(\hat{\lambda}_+) \mid \{Z_{1:n+1}\} = \{z_{1:n+1}\}] &\leq \alpha + \frac{K}{n+1} \sum_{i=1}^{n+1} \epsilon_i. \end{aligned}$$

Then, marginalizing over the event and applying ϵ -replace-one stability, we have

$$\mathbb{E}[L_{n+1}(\hat{\lambda}_+)] \leq \alpha + K\epsilon.$$

Note that the above analysis also applies for any alternative $\hat{\lambda}'_+$ that is a deterministic function of $\{l_{1:n}\}$ and where almost surely $\hat{\lambda}'_+ \geq \lambda_+$, and assuming, $\hat{\lambda}'_+$ is ϵ -replace-one stable. □

B.2. Proof for Conformal Policy Control Guarantee

Notation:

- **Data (sequences of random variables and observed values):** For all $i \in \mathbb{N}$, denote the random variable for the i -th data sample as $Z_i \in \mathcal{Z}$, and denote observed value of that random variable in lower case as $z_i \in \mathcal{Z}$. For example, we might have $\mathcal{Z} = \mathcal{X} \times \mathcal{A} \times \mathbb{R} \times \mathbb{R}$ if $Z = (X, A, R, L)$ is a vector of context, action, reward, and loss. Similarly, denote a sequence of random variables as $Z_{1:m} := (Z_1, \dots, Z_m)$ and a sequence of observed data values as $z_{1:m} := (z_1, \dots, z_m)$ for any $m \in \mathbb{N}$. To concisely denote indices, let $[m] := \{1, \dots, m\}$.
- **Hyperparameters:** Let \mathbb{R} be the space of hyperparameters, and let $\beta \in \mathbb{R}$ denote a particular hyperparameter.
- **Loss functions:** For some real-valued function $g : \mathcal{Z} \times \mathbb{R} \rightarrow \mathbb{R}$, and for all $\beta \in \mathbb{R}$ and all $i \in \mathbb{N}$, let $L_i(\beta) := g(Z_i, \beta)$ denote the loss function determined by a random variable Z_i and parameter $\beta \in \mathbb{R}$, and let $\ell_i := g(z_i, \beta)$ denote the loss function determined by the observed value z_i and parameter $\beta \in \mathbb{R}$. Note that allowing the loss functions to be a function of β does not preclude the setting where the losses are independent of β , that is where $L_i(\beta) = L_i$ for all $\beta \in \mathbb{R}$ (i.e., where changing β does not change the loss). Such a setting motivates allowing β to parameterize the policies.

- **Bags:** For any sequence $v_{1:m} := (v_1, \dots, v_m)$, let $\wr v_{1:m} \wr$ denote the *bag* (or multiset) containing the values of that sequence $v_{1:m}$ (but importantly, $\wr v_{1:m} \wr$ does *not* contain the information about the order of $v_{1:m}$). For example, $\wr (1, 7, 42, 7) \wr$ conveys that there is one 1, two 7s, and one 42 in the bag, but it does *not* convey the order that these appeared in the sequence $(1, 7, 42, 7)$. In particular, with this notation, for the random variables $Z_{1:m}$, let $\wr Z_{1:m} \wr$ denote the bag containing those random variables; for observed values $z_{1:m}$, let $\wr z_{1:m} \wr$ denote the bag containing those observed values; and thus $\wr Z_{1:m} \wr = \wr z_{1:m} \wr$ denotes the event of observing $\wr z_{1:m} \wr$, in other words, that each Z_i takes a different value in $\wr z_{1:m} \wr$, but it is not yet known *which* value (for all $i \in [m]$).
- **Policies (Distributions):** Let $\pi_{1:m} := \pi_{Z_1, \dots, Z_m}$ denote the policy or joint density function⁷ for Z_1, \dots, Z_m , and let $\pi_{\wr Z_{1:m} \wr} := \pi_{\wr Z_1, \dots, Z_m \wr}$ denote the (pushforward) distribution induced by the mapping $(z_0, \dots, z_m) \rightarrow \wr z_{1:m} \wr$.

Theorem B.2 (Restatement of Theorem 4.5). *Assume that $\mathbb{E}_{\pi_0}[L_t] \leq \alpha$, $L_i \in [0, B]$, $B < \infty$ for all i , and $\hat{\beta}$ is ϵ -replace-one stable. If $w_i^{(\hat{\beta})}$ is K -Lipschitz in β for all i , then*

$$\mathbb{E}_{\pi_{0:t}^{(\hat{\beta})}}[L_t] \leq \alpha + BK\epsilon.$$

If $(l_i - \alpha) \cdot w_i^{(\hat{\beta})}$ is K' -Lipschitz in β , then

$$\mathbb{E}_{\pi_{0:t}^{(\hat{\beta})}}[L_t] \leq \alpha + K'\epsilon.$$

Proof.

For ease of notation, we conduct the proof in an online setting where only one action is taken (or sample is generated) at each policy improvement step. This will allow the indices $t = 0, 1, \dots$ to denote both the timestep of policy improvement and the timestep of the action/sample, but the result will hold generally for a batch setting too (with the guarantee still holding marginally over the whole procedure).

We proceed by induction. For $t = 0$, we assumed access to a safe initial policy, π_0 , satisfying our risk control criterion. That is, we assume

$$\mathbb{E}_{Z_0 \sim \pi_0}[L_0] \leq \alpha.$$

Now, for the induction hypothesis assume that risk control holds at time $t - 1$, that is, assume

$$\mathbb{E}_{Z_{0:t-1} \sim \pi_{0:t-1}^{(\hat{\beta}_1: \hat{\beta}_{t-1})}}[L_{t-1}] \leq \alpha.$$

We then want to show that risk control also holds at time t :

$$\mathbb{E}_{Z_{0:t} \sim \pi_{0:t}^{(\hat{\beta}_1: \hat{\beta}_t)}}[L_t] \leq \alpha,$$

where note that $\pi_{0:t}^{(\hat{\beta}_t)}(z_{0:t}) = \pi_t^{(\hat{\beta}_t)}(z_t | z_{0:t-1})\pi_{0:t-1}^{(\hat{\beta}_1: \hat{\beta}_{t-1})}(z_{0:t-1})$. Note that at time t , we will only consider tuning $\hat{\beta}_t$, and we treat $\hat{\beta}_1, \dots, \hat{\beta}_{t-1}$ as previously tuned. Accordingly, to lighten notation, we hereon denote the expectation we wish to bound as $\mathbb{E}_{\pi_{0:t}^{(\hat{\beta})}}[L_t] := \mathbb{E}_{Z_{0:t} \sim \pi_{0:t}^{(\hat{\beta}_1: \hat{\beta}_t)}}[L_t]$, where note that we also let $\hat{\beta} := \hat{\beta}_t$.

For any control parameter β , any policies $\pi_{0:t}^{(\beta)}$, and any bag of data $\wr z_{0:t} \wr$, following Tibshirani et al. (2019); Prinster et al. (2024) define the oracle normalized conformal weights as

$$\tilde{w}_i^{(\beta)} := \tilde{w}_i(\pi_{0:t}^{(\beta)}, \wr z_{0:t} \wr) = \mathbb{P}_{\pi_{0:t}^{(\beta)}}(Z_t = z_i | \wr z_{0:t} \wr) = \frac{\sum_{\sigma: \sigma(t)=i} \pi_{0:t}^{(\beta)}(z_{\sigma(0)}, \dots, z_{\sigma(t)})}{\sum_{\sigma} \pi_{0:t}^{(\beta^*)}(z_{\sigma(0)}, \dots, z_{\sigma(t)})} \quad (17)$$

for all $i \in \{0, \dots, t\}$, as well as the unnormalized weights,

$$w_i^{(\beta)} := w_i(\pi_{0:t}^{(\beta)}, \wr z_{0:t} \wr) = \sum_{\sigma: \sigma(t)=i} \pi_{0:t}^{(\beta)}(z_{\sigma(0)}, \dots, z_{\sigma(t)}), \quad (18)$$

⁷In a slight abuse of notation for the policy control setting, we do not distinguish between CDFs and density functions here.

so note that $\tilde{w}_i^{(\beta)} = \frac{w_i^{(\beta)}}{\sum_{i=0}^t w_i^{(\beta)}}$, and define the vector $\tilde{w}_{0:t}^{(\beta)} := (\tilde{w}_0^{(\beta)}, \dots, \tilde{w}_t^{(\beta)})$.

Also define the conservative (normalized) weight for an unknown test point as

$$\tilde{w}_{\max}^{(\beta)} := \sup_{z_t \in \mathcal{Z}} (\tilde{w}_t^{(\beta)}).$$

Assume there is some small, positive $\beta_{\min} \ll 1$ such that $\beta_{\min} \leq \pi_t(x)/\pi_0(x)$ for all $x \in \mathcal{X}$. This is the safe hyperparameter value, for which $\pi_t^{(\beta_{\min})} = \pi_0$.

Step 0: Law of total expectation over draw of bag.

Expanding $\mathbb{E}_{\pi_{0:t}^{(\hat{\beta})}} [L_t]$ via the law of total expectation over the event $\{Z_{0:t} = z_{0:t}\}$, we have

$$\mathbb{E}_{\pi_{0:t}^{(\hat{\beta})}} [L_t] = \mathbb{E} \left[\mathbb{E}_{\pi_{0:t}^{(\hat{\beta})}} [L_t \mid \{Z_{0:t} = z_{0:t}\}] \right]. \quad (19)$$

We can thus see that, to prove the desired result, it is sufficient to upper bound $\mathbb{E}_{\pi_{0:t}^{(\hat{\beta})}} [L_t \mid \{Z_{0:t} = z_{0:t}\}]$ almost surely given any draw of the bag, $\{Z_{0:t}\}$.

Step 1: Deterministic inequalities on bag-conditional risks.

Define the following family of hyperparameters:

$$\hat{\beta}(\{l_{1:m}\}, \tilde{w}_{1:m}^{(\cdot)}, \gamma) = \sup \left\{ \beta' \in \beta \quad : \quad \forall \quad \beta \leq \beta', \quad \sum_{i=1}^m l_i \cdot \tilde{w}_i^{(\beta)} \leq \gamma \right\}.$$

When the set is empty, define $\hat{\beta}(\{l_{1:m}\}, \tilde{w}_{1:m}^{(\cdot)}, \gamma) = \beta_{\min}$.

By the continuity of $\tilde{w}_i^{(\cdot)}$ (and $L_i(\cdot)$) for all $i \in \mathbb{N}$, the sum $\sum_{i=1}^m l_i \cdot \tilde{w}_i^{(\beta)}$ is right-continuous for any $Z_{1:m}$, which gives us the following deterministic inequality for any γ :

$$\sum_{i=1}^m l_i \cdot \tilde{w}_i^{(\beta)} \leq \gamma \quad \forall \quad \beta \leq \hat{\beta}(\{L_{1:m}\}, \tilde{w}_{1:m}^{(\cdot)}, \gamma). \quad (20)$$

Step 2: Showing an oracle procedure deterministically controls the bag-conditional risk.

Using the family of thresholds we defined above and applying it to the bag of loss functions for both the calibration set and the test point, define the oracle threshold as

$$\beta^* := \hat{\beta}(\{L_{0:t}\}, \tilde{w}_{0:t}^{(\cdot)}, \alpha). \quad (21)$$

Now, consider the quantity $\mathbb{E}_{\pi_{0:t}^{(\beta^*)}} [L_t \mid \{Z_{0:t} = z_{0:t}\}]$, which we can view as the bag-conditional oracle risk. That is, we can interpret this quantity as the expected value, with respect to the policy $\pi_{0:t}^{(\beta^*)}$, that the random variable L_t will take on, given the bag of data $\{z_{0:t}\}$. Note that conditioning on the bag of data, $\{z_{0:t}\}$, implies the event of observing the bag of loss functions, $\{l_{0:t}\}$,⁸ which thereby determines the value of β^* , since β^* is a function of $\{z_{0:t}\}$ (as well as the policy, $\pi_{0:t}^{(\cdot)}$, and the constraint function g).

⁸That is, implies the event $\{L_1, \dots, L_t\} = \{l_1, \dots, l_t\}$, because the loss functions are defined as $l_i := g(z_i)$ for all $i \in \mathbb{N}$.

Using the definition of conditional expectation, and secondly using the definition of conditional probability, we have

$$\begin{aligned}\mathbb{E}_{\pi_{0:t}^{(\beta^*)}} [L_t \mid \mathcal{Z}_{0:t} = \mathcal{z}_{0:t}] &= \sum_{i=0}^t l_i \cdot \mathbb{P}(Z_t = z_i \mid \mathcal{Z}_{0:t} = \mathcal{z}_{0:t}) \\ &= \sum_{i=0}^t l_i \cdot \frac{\mathbb{P}(Z_t = z_i, \mathcal{Z}_{0:t} = \mathcal{z}_{0:t})}{\mathbb{P}(\mathcal{Z}_{0:t} = \mathcal{z}_{0:t})}.\end{aligned}$$

Applying the law of total probability over permutations ($\sigma : \{0, \dots, t\} \rightarrow \{0, \dots, t\}$) to the probabilities in the numerator and denominator of the RHS, we have

$$\begin{aligned}\mathbb{E}_{\pi_{0:t}^{(\beta^*)}} [L_t \mid \mathcal{Z}_{0:t} = \mathcal{z}_{0:t}] &= \sum_{i=0}^t l_i \cdot \frac{\sum_{\sigma: \sigma(t)=i} \pi_{0:t}^{(\beta^*)}(z_{\sigma(0)}, \dots, z_{\sigma(t)})}{\sum_{\sigma} \pi_{0:t}^{(\beta^*)}(z_{\sigma(0)}, \dots, z_{\sigma(t)})} \\ &= \sum_{i=0}^t l_i \cdot \tilde{w}_i^{(\beta^*)}\end{aligned}$$

Now, using Eq. (20),

$$\sum_{i=0}^t l_i \cdot \tilde{w}_i^{(\beta)} \leq \alpha \quad \forall \quad \text{fixed } \beta \leq \beta^*, \quad (22)$$

where here by “fixed” we mean that β is constant conditional on the bag of data, $\mathcal{Z}_{0:t} = \mathcal{z}_{0:t}$.

Step 3: Relating the empirically-selected hyperparameter to the oracle parameter

In Step 2, we have shown that an oracle procedure deterministically controls the risk, conditional on the event $\mathcal{Z}_{0:t} = \mathcal{z}_{0:t}$. However, this oracle procedure cannot be implemented in practice due to requiring knowledge of the test point loss, L_t , as well as the weight assigned to the test point (as a function of β), \tilde{w}_t ; that is, recall we defined $\beta^* := \hat{\beta}(\mathcal{L}_{0:t}, \tilde{w}_{0:t}^{(\cdot)}, \alpha)$. In this next step of the proof we would now like to prove a deterministic relationship between the oracle parameter, β^* , and the empirically-selected parameter, $\hat{\beta} := \hat{\beta}(\mathcal{L}_{1:t-1}, B, \tilde{w}_{0:t-1}^{(\cdot)}, \tilde{w}_{\max}^{(\cdot)}, \alpha)$, to conclude valid risk control for the empirical method; that is, we would like to deterministically show $\beta^* \geq \hat{\beta}$.

To begin, recall that in Step 2, conditioning on the event $\mathcal{Z}_{0:t} = \mathcal{z}_{0:t}$ implied that $\hat{\beta}(\mathcal{L}_{0:t}, \tilde{w}_{0:t}^{(\cdot)}, \alpha) = \hat{\beta}(\mathcal{l}_{0:t}, \tilde{w}_{0:t}^{(\cdot)}, \alpha)$. For the empirical parameter, however, conditioning on $\mathcal{Z}_{0:t} = \mathcal{z}_{0:t}$ does *not* imply what may seem analogous: that is, it could be that $\hat{\beta}(\mathcal{L}_{0:t-1}, B, \tilde{w}_{0:t-1}^{(\cdot)}, \tilde{w}_{\max}^{(\cdot)}, \alpha) \neq \hat{\beta}(\mathcal{l}_{0:t-1}, B, \tilde{w}_{0:t-1}^{(\cdot)}, \tilde{w}_{\max}^{(\cdot)}, \alpha)$. This is because the event $\mathcal{Z}_{0:t} = \mathcal{z}_{0:t}$ only allows us to conclude that the $t-1$ random variables in $\mathcal{L}_{1:t-1}$ take $t-1$ distinct values from the bag of t observed losses, $\mathcal{l}_{0:t}$, but we do not yet know *which* observed losses. That is, what we *can* conclude is, given $\mathcal{Z}_{0:t} = \mathcal{z}_{0:t}$, that

$$\mathcal{Z}_{0:t} = \mathcal{z}_{0:t} \implies \mathcal{L}_{1:t-1} \in \left\{ \mathcal{l}_{0:t \setminus i} \right\}_{i \in \{0, \dots, t\}},$$

where $\mathcal{l}_{0:t \setminus i} := \mathcal{l}_{0:t} \setminus \{l_i\}$. Accordingly, conditioning on the event $\mathcal{Z}_{0:t} = \mathcal{z}_{0:t}$ implies the following equivalence:

$$\beta^* \geq \hat{\beta}(\mathcal{L}_{0:t-1}, B, \tilde{w}_{0:t-1}^{(\cdot)}, \tilde{w}_{\max}^{(\cdot)}, \alpha) \text{ almost surely} \iff \beta^* \geq \hat{\beta}(\mathcal{l}_{0:t \setminus i}, B, \tilde{w}_{0:t-1}^{(\cdot)}, \tilde{w}_{\max}^{(\cdot)}, \alpha) \quad \forall \quad i \in \{0, \dots, t\}. \quad (23)$$

So, we will focus on proving the latter.

Recall that we have assumed that l is bounded above by B , for any $\beta \in \mathbb{R}$, and by the definition of $\tilde{w}_{\max}^{(\cdot)}$, deterministically we have

$$\sum_{j \in \{0, \dots, t\}} l_j \cdot \tilde{w}_j^{(\beta)} \leq B \cdot \tilde{w}_{\max}^{(\beta)} + \sum_{j \in \{0, \dots, t\} \setminus i} l_j \cdot \tilde{w}_j^{(\beta)} \quad \forall \quad i \in \{0, \dots, t\}, \quad (24)$$

where the right-hand side of the above inequalities can be interpreted as a conservative risk obtained by replacing l_i with the bound B .

Thus, for any β , we can use (24) to conclude

$$B \cdot \tilde{w}_{\max}^{(\beta)} + \sum_{j \in \{0, \dots, t\} \setminus i} l_j \cdot \tilde{w}_i^{(\beta)} \leq \alpha \implies \sum_{j \in \{0, \dots, t\}} l_j \cdot \tilde{w}_j^{(\beta)} \leq \alpha \quad \forall \quad i \in \{0, \dots, t\}. \quad (25)$$

So, by Eq. (25) and the definition of $\hat{\beta}(\mathcal{I}_{0:t \setminus i}, B)$, it must hold that

$$\beta^* \geq \hat{\beta}(\mathcal{I}_{0:t \setminus i}, B), \tilde{w}_{0:t-1}^{(\cdot)}, \tilde{w}_{\max}^{(\cdot)}, \alpha) \quad \forall \quad i \in \{0, \dots, t\}. \quad (26)$$

Step 4: Analyzing the bag-conditional risk of the empirical procedure via Lipschitz continuity

Now we turn to plugging the empirical algorithm's hyperparameter into the bag-conditional risk, and then analyzing this risk using Lipschitz continuity and a type of stability called "replace-one" stability. This analysis is necessary because $\hat{\beta} = \hat{\beta}(\mathcal{I}_{0:t-1}, B), \tilde{w}_{0:t-1}^{(\cdot)}, \tilde{w}_{\max}^{(\cdot)}, \alpha)$ is not constant conditional on $\mathcal{I}_{Z_{0:t}} = \mathcal{I}_{z_{0:t}}$, so Eq. (22) would not directly apply.

Begin by expanding the quantity $\mathbb{E}_{\pi_{0:t}^{(\hat{\beta})}} [L_t \mid \mathcal{I}_{Z_{0:t}} = \mathcal{I}_{z_{0:t}}]$ by LOTE over the event $Z_t = z_i$:

$$\begin{aligned} & \mathbb{E}_{\pi_{0:t}^{(\hat{\beta})}} [L_t \mid \mathcal{I}_{Z_{0:t}} = \mathcal{I}_{z_{0:t}}] \\ &= \mathbb{E}_{\pi_{0:t}^{(\hat{\beta})}} \left[\mathbb{E}_{\pi_{0:t}^{(\hat{\beta})}} [L_t \mid \mathcal{I}_{Z_{0:t}} = \mathcal{I}_{z_{0:t}}, Z_t = z_i] \mid \mathcal{I}_{Z_{0:t}} = \mathcal{I}_{z_{0:t}} \right] \\ &= \sum_{i=0}^t \mathbb{E}_{\pi_{0:t}^{(\hat{\beta})}} [L_t \mid \mathcal{I}_{Z_{0:t}} = \mathcal{I}_{z_{0:t}}, Z_t = z_i] \cdot \mathbb{P}_{\pi_{0:t}^{(\hat{\beta})}} (Z_t = z_i \mid \mathcal{I}_{Z_{0:t}} = \mathcal{I}_{z_{0:t}}) \\ &= \sum_{i=0}^t l_i \cdot \mathbb{P}_{\pi_{0:t}^{(\hat{\beta})}} (Z_t = z_i \mid \mathcal{I}_{Z_{0:t}} = \mathcal{I}_{z_{0:t}}). \end{aligned} \quad (27)$$

Writing out the conditional probability in Eq. (27) using the definition of conditional probability, and then (in both the numerator and denominator) the law of total probability and chain rule,

$$\begin{aligned} & \mathbb{P}_{\pi_{0:t}^{(\hat{\beta})}} (Z_t = z_i \mid \mathcal{I}_{Z_{0:t}} = \mathcal{I}_{z_{0:t}}) \\ &= \frac{\sum_{\sigma: \sigma(t)=i} \pi_{0:t}^{(\hat{\beta})} (z_{\sigma(0)}, \dots, z_{\sigma(t)})}{\sum_{\sigma} \pi_{0:t}^{(\hat{\beta})} (z_{\sigma(0)}, \dots, z_{\sigma(t)})} \\ &= \frac{\sum_{\sigma: \sigma(t)=i} \pi_{t|0:t-1}^{(\hat{\beta})} (z_{\sigma(t)} \mid z_{\sigma(0)}, \dots, z_{\sigma(t-1)}) \cdot \pi_{t-1|0:t-2} (z_{\sigma(t-1)} \mid z_{\sigma(0)}, \dots, z_{\sigma(t-2)}) \cdots \pi_0 (z_{\sigma(0)})}{\sum_{\sigma} \pi_{t|0:t-1}^{(\hat{\beta})} (z_{\sigma(t)} \mid z_{\sigma(0)}, \dots, z_{\sigma(t-1)}) \cdot \pi_{t-1|0:t-2} (z_{\sigma(t-1)} \mid z_{\sigma(0)}, \dots, z_{\sigma(t-2)}) \cdots \pi_0 (z_{\sigma(0)})}, \end{aligned}$$

and by expanding the summation in the denominator, this is equivalent to

$$\begin{aligned} & \mathbb{P}_{\pi_{0:t}^{(\hat{\beta})}} (Z_t = z_i \mid \mathcal{I}_{Z_{0:t}} = \mathcal{I}_{z_{0:t}}) \\ &= \frac{\sum_{\sigma: \sigma(t)=i} \pi_{t|0:t-1}^{(\hat{\beta})} (z_{\sigma(t)} \mid z_{\sigma(0)}, \dots, z_{\sigma(t-1)}) \cdot \pi_{t-1|0:t-2} (z_{\sigma(t-1)} \mid z_{\sigma(0)}, \dots, z_{\sigma(t-2)}) \cdots \pi_0 (z_{\sigma(0)})}{\sum_i \sum_{\sigma: \sigma(t)=i} \pi_{t|0:t-1}^{(\hat{\beta})} (z_{\sigma(t)} \mid z_{\sigma(0)}, \dots, z_{\sigma(t-1)}) \cdot \pi_{t-1|0:t-2} (z_{\sigma(t-1)} \mid z_{\sigma(0)}, \dots, z_{\sigma(t-2)}) \cdots \pi_0 (z_{\sigma(0)})}. \end{aligned}$$

In this expanded form, examine the factor $\pi_{t|0:t-1}^{(\hat{\beta})} (z_{\sigma(t)} \mid z_{\sigma(0)}, \dots, z_{\sigma(t-1)})$, and recalling that $\hat{\beta} := \hat{\beta}(\mathcal{I}_{0:t-1}, B), \tilde{w}_{0:t-1}^{(\cdot)}, \tilde{w}_{\max}^{(\cdot)}, \alpha)$, note that the conditioning on $z_{\sigma(0)}, \dots, z_{\sigma(t-1)}$ inside the summation $\sum_{\sigma: \sigma(t)=i}$, where

the permutations are $\sigma : \sigma(t) = i$, implies $Z_t = z_{\sigma(t)} = z_i \implies \mathcal{L}_{0:t-1} = \mathcal{L}_{0:t-1}^i$ (that is, implies a specific realization of $\mathcal{L}_{0:t-1}$ among t possible bags of observed losses). Accordingly, let us denote $\hat{\beta}^i := \hat{\beta}(\mathcal{L}_{0:t-1}^i, B, \tilde{w}_{0:t-1}^{(\cdot)}, \tilde{w}_{\max}^{(\cdot)}, \alpha)$. Then, note that the numerator and the analogous inner summation in the denominator are the unnormalized weights in Eq. (18), that is, we can concisely write those summations as $\sum_{\sigma: \sigma(t)=i}(\dots) = w_i^{(\hat{\beta}^i)}$. That is, we have

$$\mathbb{P}_{\pi_{0:t}^{(\hat{\beta})}}(Z_t = z_i \mid \mathcal{L}_{0:t} = \mathcal{L}_{0:t}^i) = \frac{w_i^{(\hat{\beta}^i)}}{\sum_j w_j^{(\hat{\beta}^j)}}. \quad (28)$$

Plugging this into Eq. (27), we have

$$\mathbb{E}_{\pi_{0:t}^{(\hat{\beta})}}[L_t \mid \mathcal{L}_{0:t} = \mathcal{L}_{0:t}^i] = \sum_{i=0}^t l_i \cdot \frac{w_i^{(\hat{\beta}^i)}}{\sum_j w_j^{(\hat{\beta}^j)}} = \frac{1}{\sum_j w_j^{(\hat{\beta}^j)}} \sum_{i=0}^t l_i \cdot w_i^{(\hat{\beta}^i)} \quad (29)$$

Importantly, note that in Eq. (29), which can be viewed as the true bag-conditional risk of the empirical algorithm, that the unnormalized weight in the numerator, $w_i^{(\hat{\beta}^i)}$, differs for each loss function, l_i , in the summation, and moreover the same is true in the denominator's summation, which is why we cannot apply Eq. (22) to bound it directly.

Instead, we now move toward relating Eq. (29) and Eq. (22) using Lipschitz continuity and the replace-one (in)stability of the algorithm. However, although in the analogous step assuming parameterized losses (Section B.1) we were able to directly apply Lipschitz continuity at this stage, here we must be more careful. That is, although in Section B.1 we could conservatively assume that each replace-one perturbation ϵ_i increased its corresponding loss by at most $K\epsilon_i$, a subtle difference here is that if we artificially increased the unnormalized weight of certain (e.g., smaller-loss) indices by some amount, this may *decrease* the overall bag-conditional weighted risk after re-normalizing the probability weights, and thus not result in a valid upper bound. In other words, conservative estimates of losses monotonically result in conservative estimates of the risk (in Section B.1), but here, conservative estimates of (unnormalized) weights introduce an additional source of non-monotonicity that may not result in a conservative estimate of the weighted (bag-conditional) risk.

For all $i \in [n]$, denote the magnitude of perturbation to the hyperparameter $\hat{\beta}(\mathcal{L}_{0:t-1}^i, B, \tilde{w}_{0:t-1}^{(\cdot)}, \tilde{w}_{\max}^{(\cdot)}, \alpha)$ caused by replacing the loss function l_i with l_t as

$$\begin{aligned} \epsilon_i &= \left| \hat{\beta}(\mathcal{L}_{0:t-1}, B, \tilde{w}_{0:t-1}^{(\cdot)}, \tilde{w}_{\max}^{(\cdot)}, \alpha) - \hat{\beta}(\mathcal{L}_{0:t-1}^i, B, \tilde{w}_{0:t-1}^{(\cdot)}, \tilde{w}_{\max}^{(\cdot)}, \alpha) \right| \\ &= \left| \hat{\beta}^t - \hat{\beta}^i \right|. \end{aligned}$$

Making the substitution $w_i^{(\hat{\beta}^i)} = w_i^{(\hat{\beta}^t)} + (w_i^{(\hat{\beta}^i)} - w_i^{(\hat{\beta}^t)})$ in Eq. (29) and then rearranging terms, we have

$$\begin{aligned} \mathbb{E}_{\pi_{0:t}^{(\hat{\beta})}}[L_t \mid \mathcal{L}_{0:t} = \mathcal{L}_{0:t}^i] &= \frac{1}{\sum_j w_j^{(\hat{\beta}^j)}} \sum_{i=0}^t l_i \cdot w_i^{(\hat{\beta}^t)} + (l_i \cdot w_i^{(\hat{\beta}^i)} - l_i \cdot w_i^{(\hat{\beta}^t)}) \\ &= \frac{1}{\sum_j w_j^{(\hat{\beta}^j)}} \sum_{i=0}^t l_i \cdot w_i^{(\hat{\beta}^t)} + \frac{1}{\sum_j w_j^{(\hat{\beta}^j)}} \sum_{i=0}^t (l_i \cdot w_i^{(\hat{\beta}^i)} - l_i \cdot w_i^{(\hat{\beta}^t)}). \end{aligned}$$

Now multiplying the first term by $1 = \frac{\sum_j w_j^{(\hat{\beta}^t)}}{\sum_j w_j^{(\hat{\beta}^j)}}$,

$$\begin{aligned} \mathbb{E}_{\pi_{0:t}^{(\hat{\beta})}}[L_t \mid \mathcal{L}_{0:t} = \mathcal{L}_{0:t}^i] &= \frac{\sum_j w_j^{(\hat{\beta}^t)}}{\sum_j w_j^{(\hat{\beta}^j)}} \frac{1}{\sum_j w_j^{(\hat{\beta}^j)}} \sum_{i=0}^t l_i \cdot w_i^{(\hat{\beta}^t)} + \frac{1}{\sum_j w_j^{(\hat{\beta}^j)}} \sum_{i=0}^t (l_i \cdot w_i^{(\hat{\beta}^i)} - l_i \cdot w_i^{(\hat{\beta}^t)}) \\ &= \frac{\sum_j w_j^{(\hat{\beta}^t)}}{\sum_j w_j^{(\hat{\beta}^j)}} \sum_{i=0}^t \frac{l_i \cdot w_i^{(\hat{\beta}^t)}}{\sum_j w_j^{(\hat{\beta}^j)}} + \frac{1}{\sum_j w_j^{(\hat{\beta}^j)}} \sum_{i=0}^t (l_i \cdot w_i^{(\hat{\beta}^i)} - l_i \cdot w_i^{(\hat{\beta}^t)}), \end{aligned}$$

Then by Eq. (22), we know that $\sum_{i=0}^t \frac{l_i \cdot w_i^{(\hat{\beta}^{\setminus t})}}{\sum_j w_j^{(\hat{\beta}^{\setminus t})}} \leq \alpha$ (note that $\hat{\beta}^{\setminus t}$ is fixed with respect to the summations in the term), so

$$\mathbb{E}_{\pi_{0:t}^{(\hat{\beta})}} \left[L_t \mid \{Z_{0:t}\} = \{z_{0:t}\} \right] \leq \frac{\sum_j w_j^{(\hat{\beta}^{\setminus t})}}{\sum_j w_j^{(\hat{\beta}^{\setminus j})}} \cdot \alpha + \frac{1}{\sum_j w_j^{(\hat{\beta}^{\setminus j})}} \sum_{i=0}^t (l_i \cdot w_i^{(\hat{\beta}^{\setminus i})} - l_i \cdot w_i^{(\hat{\beta}^{\setminus t})}). \quad (30)$$

Plugging in $w_j^{(\hat{\beta}^{\setminus t})} = w_j^{(\hat{\beta}^{\setminus j})} + (w_j^{(\hat{\beta}^{\setminus j})} - w_j^{(\hat{\beta}^{\setminus j})})$ into the numerator of the first term of the RHS of (30) and rearranging terms,

$$\begin{aligned} & \frac{\sum_j w_j^{(\hat{\beta}^{\setminus t})}}{\sum_j w_j^{(\hat{\beta}^{\setminus j})}} \cdot \alpha + \frac{1}{\sum_j w_j^{(\hat{\beta}^{\setminus j})}} \sum_{i=0}^t (l_i \cdot w_i^{(\hat{\beta}^{\setminus i})} - l_i \cdot w_i^{(\hat{\beta}^{\setminus t})}) \\ &= \frac{\sum_j (w_j^{(\hat{\beta}^{\setminus t})} + w_j^{(\hat{\beta}^{\setminus j})} - w_j^{(\hat{\beta}^{\setminus j})})}{\sum_j w_j^{(\hat{\beta}^{\setminus j})}} \cdot \alpha + \frac{1}{\sum_j w_j^{(\hat{\beta}^{\setminus j})}} \sum_{i=0}^t (l_i \cdot w_i^{(\hat{\beta}^{\setminus i})} - l_i \cdot w_i^{(\hat{\beta}^{\setminus t})}) \\ &= \alpha + \frac{\sum_j (w_j^{(\hat{\beta}^{\setminus t})} - w_j^{(\hat{\beta}^{\setminus j})}) \cdot \alpha}{\sum_j w_j^{(\hat{\beta}^{\setminus j})}} + \frac{\sum_{i=0}^t (l_i \cdot w_i^{(\hat{\beta}^{\setminus i})} - l_i \cdot w_i^{(\hat{\beta}^{\setminus t})})}{\sum_j w_j^{(\hat{\beta}^{\setminus j})}} \\ &= \alpha + \frac{\sum_{i=0}^t \alpha \cdot w_i^{(\hat{\beta}^{\setminus t})} - \alpha \cdot w_i^{(\hat{\beta}^{\setminus i})} + l_i \cdot w_i^{(\hat{\beta}^{\setminus i})} - l_i \cdot w_i^{(\hat{\beta}^{\setminus t})}}{\sum_j w_j^{(\hat{\beta}^{\setminus j})}} \\ &= \alpha + \frac{\sum_{i=0}^t l_i \cdot (w_i^{(\hat{\beta}^{\setminus i})} - w_i^{(\hat{\beta}^{\setminus t})}) - \alpha \cdot (w_i^{(\hat{\beta}^{\setminus i})} - w_i^{(\hat{\beta}^{\setminus t})})}{\sum_j w_j^{(\hat{\beta}^{\setminus j})}} \\ &= \alpha + \frac{\sum_{i=0}^t (l_i - \alpha) \cdot (w_i^{(\hat{\beta}^{\setminus i})} - w_i^{(\hat{\beta}^{\setminus t})})}{\sum_j w_j^{(\hat{\beta}^{\setminus j})}}. \end{aligned} \quad (31)$$

Note that $(l_i - \alpha) \leq B$, so we obtain the inequality

$$\frac{\sum_j w_j^{(\hat{\beta}^{\setminus t})}}{\sum_j w_j^{(\hat{\beta}^{\setminus j})}} \cdot \alpha + \frac{1}{\sum_j w_j^{(\hat{\beta}^{\setminus j})}} \sum_{i=0}^t (l_i \cdot w_i^{(\hat{\beta}^{\setminus i})} - l_i \cdot w_i^{(\hat{\beta}^{\setminus t})}) \leq \alpha + B \frac{\sum_{i=0}^t (w_i^{(\hat{\beta}^{\setminus i})} - w_i^{(\hat{\beta}^{\setminus t})})}{\sum_j w_j^{(\hat{\beta}^{\setminus j})}}. \quad (32)$$

Assuming that $w_i^{(\beta)}$ is K -Lipschitz in β , we can bound the RHS of Eq. (32) as

$$\alpha + B \frac{\sum_{i=0}^t (w_i^{(\hat{\beta}^{\setminus i})} - w_i^{(\hat{\beta}^{\setminus t})})}{\sum_j w_j^{(\hat{\beta}^{\setminus j})}} \leq \alpha + B \frac{\sum_{i=0}^t K \epsilon_i}{\sum_j w_j^{(\hat{\beta}^{\setminus j})}}. \quad (33)$$

Using transitive property across Inequality (30), Equation (31), Inequality (32), and Inequality (33), we have

$$\mathbb{E}_{\pi_{0:t}^{(\hat{\beta})}} \left[L_t \mid \{Z_{0:t}\} = \{z_{0:t}\} \right] \leq \alpha + BK \frac{\sum_{i=0}^t \epsilon_i}{\sum_j w_j^{(\hat{\beta}^{\setminus j})}},$$

and marginalizing over the event $\{Z_{0:t}\} = \{z_{0:t}\}$ gives

$$\mathbb{E}_{\pi_{0:t}^{(\hat{\beta})}} [L_t] \leq \alpha + BK\epsilon. \quad (34)$$

Alternatively, if from Eq. (31) we instead assumed that $(l_i - \alpha) \cdot w_i^{(\beta)}$ is K Lipschitz in β , then from Eq. (31) we obtain the inequality

$$\alpha + \frac{\sum_{i=0}^t (l_i - \alpha)(w_i^{(\hat{\beta}^{\lambda^i})} - w_i^{(\hat{\beta}^{\lambda^t})})}{\sum_j w_j^{(\hat{\beta}^{\lambda^j})}} \leq \alpha + \frac{\sum_{i=0}^t K\epsilon_i}{\sum_j w_j^{(\hat{\beta}^{\lambda^j})}}, \quad (35)$$

and using transitive property across Inequality (30), Equation (31), and Inequality (35), we have

$$\mathbb{E}_{\pi_{0:t}^{(\hat{\beta})}} [L_t \mid \mathcal{Z}_{0:t} = \mathcal{z}_{0:t}] \leq \alpha + K \frac{\sum_{i=0}^t \epsilon_i}{\sum_j w_j^{(\hat{\beta}^{\lambda^j})}},$$

and marginalizing over the event $\mathcal{Z}_{0:t} = \mathcal{z}_{0:t}$ gives

$$\mathbb{E}_{\pi_{0:t}^{(\hat{\beta})}} [L_t] \leq \alpha + K\epsilon. \quad (36)$$

□

B.3. Counterexample to GCRC risk control on arbitrary bounded losses

Proposition B.3. *The following assumptions are not sufficient for $\hat{\lambda}_+$ as defined in Eq. (4) to achieve the risk control guarantee at level α :*

- *Right-continuity of $L_i(\lambda)$ in λ ,*
- *Existence of a safe hyperparameter: For $\lambda_{\max} := \sup \Lambda \in \Lambda$, that $L_i(\lambda_{\max}) \leq \alpha$,*
- *Boundedness of the loss functions: $\sup_{\lambda} L_i(\lambda) \leq B < \infty$ almost surely.*

Proof. This counterexample assumes exchangeable data. Let $\Lambda = \{\lambda_1, \lambda_2, \lambda_3, \lambda_{\max}\}$ where $\lambda_1 < \lambda_2 < \lambda_3 < \lambda_{\max}$. Fix $\alpha \in (0, 1]$. Consider the following $n + 1 = 3$ loss functions, where $B = \frac{3}{2}\alpha$:

$$l_1(\lambda) = \begin{cases} B, & \lambda = \lambda_1 \\ B/2, & \lambda = \lambda_2 \\ 0, & \lambda = \lambda_3 \\ 0, & \lambda = \lambda_{\max} \end{cases}, \quad l_2(\lambda) = \begin{cases} B/2, & \lambda = \lambda_1 \\ B, & \lambda = \lambda_2 \\ 0, & \lambda = \lambda_3 \\ 0, & \lambda = \lambda_{\max} \end{cases}, \quad l_3(\lambda) = \begin{cases} B/2, & \lambda = \lambda_1 \\ 0, & \lambda = \lambda_2 \\ B, & \lambda = \lambda_3 \\ 0, & \lambda = \lambda_{\max} \end{cases}. \quad (37)$$

Note that $\max_{\lambda \in \Lambda} l_i(\lambda) = B$ and $l_i(\lambda_{\max}) = 0 < \alpha$ for all $i \in [3]$, satisfying our assumptions.

Consider the bag-conditional empirical risk,

$$\mathbb{E}[L_3(\hat{\lambda}) \mid \mathcal{L}_{1:3} = \mathcal{l}_{1:3}] = \mathbb{E} \left[\mathbb{E}[L_3(\hat{\lambda}) \mid \mathcal{L}_{1:3} = \mathcal{l}_{1:3}, L_3 = l_i] \mid \mathcal{L}_{1:3} = \mathcal{l}_{1:3} \right], \quad (38)$$

where the inner expectation on the righthand side conditions on the value of the bag of loss functions, $\mathcal{L}_{1:3} = \mathcal{l}_{1:3}$, and additionally on the event that the test loss takes the value of the i -th loss function in the bag, $L_3 = l_i$. Note that the

test loss at the empirical threshold, $L_3(\hat{\lambda})$, is a deterministic function of the values of $\{L_{1:3}\}$ and L_3 . Therefore, this inner expectation is simply

$$\mathbb{E} \left[L_3(\hat{\lambda}) \mid \{L_{1:3}\} = \{l_{1:3}\}, L_3 = l_i \right] = l_i(\hat{\lambda}(\{l_{1:3 \setminus i}\}, B), \alpha). \quad (39)$$

Substituting this expression for the inner expectation in Eq. (38), we can write the bag-conditional empirical risk as

$$\mathbb{E}[L_3(\hat{\lambda}) \mid \{L_{1:3}\} = \{l_{1:3}\}] = \mathbb{E}[l_i(\hat{\lambda}(\{l_{1:3 \setminus i}\}, B), \alpha) \mid \{L_{1:3}\} = \{l_{1:3}\}] = \frac{1}{3} \sum_{i=1}^3 l_i(\hat{\lambda}(\{l_{1:3 \setminus i}\}, B), \alpha). \quad (40)$$

We now calculate this quantity for the bag of loss functions given in Eqs. (37). Each case or “world” below computes one summand in the mean in Eq. (40). To simplify forthcoming calculations, note that

$$\hat{\lambda}(\{l_{1:3 \setminus i}\}, B), \alpha = \min\{\lambda' \in \Lambda : \forall \lambda \geq \lambda', \sum_{j \neq i} l_j(\lambda) \leq 3\alpha - B = 2B - B = B\}.$$

- **Case 1:** $L_3 = l_1$. We have

$$\hat{\lambda}(\{l_2, l_3, B\}, \alpha) = \min\{\lambda' \in \Lambda : \forall \lambda \geq \lambda', l_2(\lambda) + l_3(\lambda) \leq B\} \quad (41)$$

$$= \lambda_1, \quad (42)$$

so $L_3(\hat{\lambda}) = l_1(\hat{\lambda}(\{l_2, l_3, B\}, \alpha)) = l_1(\lambda_1) = B$.

- **Case 2:** $L_3 = l_2$. We have

$$\hat{\lambda}(\{l_1, l_3, B\}, \alpha) = \min\{\lambda' \in \Lambda : \forall \lambda \geq \lambda', l_1(\lambda) + l_3(\lambda) \leq B\} \quad (43)$$

$$= \lambda_2, \quad (44)$$

so $L_3(\hat{\lambda}) = l_2(\hat{\lambda}(\{l_1, l_3, B\}, \alpha)) = l_2(\lambda_2) = B$.

- **Case 3:** $L_3 = l_3$. We have

$$\hat{\lambda}(\{l_1, l_2, B\}, \alpha) = \min\{\lambda' \in \Lambda : \forall \lambda \geq \lambda', l_1(\lambda) + l_2(\lambda) \leq B\} \quad (45)$$

$$= \lambda_3, \quad (46)$$

so $L_3(\hat{\lambda}) = l_3(\hat{\lambda}(\{l_1, l_2, B\}, \alpha)) = l_3(\lambda_3) = B$.

Plugging these values into Eq. (40) gives

$$\begin{aligned} \mathbb{E}[L_3(\hat{\lambda}) \mid \{L_{1:3}\} = \{l_{1:3}\}] &= \frac{1}{3} \sum_{i=1}^3 l_i(\hat{\lambda}(\{l_{1:3 \setminus i}\}, B), \alpha) \\ &= \frac{1}{3}(B + B + B) \\ &= B = \frac{3}{2}\alpha > \alpha. \end{aligned}$$

□

B.4. Conservative adjustment to gCRC for level α validity if K is known

Assume the gCRC setting of Theorem 4.2 in Section 4.1 (although an analogous result would also hold for conformal policy control). In practice, the deviation of the empirical gCRC algorithm due to replacing one sample can be bounded above by

$$\hat{\epsilon}_i := \max_{b \in \{0, B\}} \left| \hat{\lambda}_+(\{l_{1:n}, B\}, \alpha) - \hat{\lambda}_+(\{l_{1:n \setminus i}, b, B\}, \alpha) \right|,$$

and if the Lipschitz constant for the loss functions is known, a conservative significance level can be obtained as

$$\hat{\alpha} := \sup \left(\left\{ \alpha' \leq \alpha \quad : \quad \alpha' + \frac{K}{n+1} \sum_{i=1}^{n+1} \hat{\epsilon}_i(\alpha') \leq \alpha \right\} \right).$$

Then, the procedure run at $\hat{\alpha}$ attains level α validity.

Proposition B.4. *In the gCRC setting of Theorem 4.2,*

$$\mathbb{E}[L_{n+1}(\hat{\lambda}_+(\hat{\alpha}))] \leq \alpha.$$

C. Detailed Methodology

This appendix provides implementation details for Conformal Policy Control. Section C.1 describes the calibration procedure for selecting the likelihood ratio bound β via weighted conformal prediction, including grid construction, normalization constant estimation, and conformal weighting. Section C.2 describes sampling algorithms for drawing actions from the constrained policy, including rejection sampling and Independence Metropolis-Hastings.

C.1. Conformal Calibration of β

This section details the procedure for calibrating the likelihood ratio bound β via weighted conformal risk control. We first define the likelihood ratio and describe how to construct a grid of candidate values (Section C.1.1). We then show how to estimate the normalization constant $\psi(\beta)$ for each candidate via importance-weighted Monte Carlo integration (Section C.1.2). Finally, we describe the conformal weighting scheme that accounts for distribution shift between calibration and deployment, and the criterion for selecting the largest β that controls risk at level α (Section C.1.3).

Remark C.1. Throughout this section we write π_0 for the reference policy used in the likelihood ratio, which generalizes π_0 from the main text: π_0 may be the initial safe policy π_0 or the previous constrained policy $\pi_{t-1}^{(\beta_{t-1})}$. We also assume a fixed context distribution $p(X)$ shared by the safe and optimized policies. Under this assumption, the context marginal cancels in the likelihood ratio $\pi_t(A_i | X_i)/\pi_0(A_i | X_i)$, and it suffices to work with conditional densities evaluated at the same context X_i .

C.1.1. LIKELIHOOD RATIOS AND GRID PREPARATION

For each action x , define the likelihood ratio

$$\text{LR}(x) := \frac{\pi_t(x)}{\pi_0(x)}, \quad (47)$$

where π_t is the current unconstrained policy and π_0 is either the initial policy π_0 or the previous constrained policy $\pi_{t-1}^{(\beta_{t-1})}$.

To calibrate β , we require two sets of samples:

- **Calibration data** \mathcal{D}_{cal} : samples from previous rounds with feasibility labels, used to compute conformal weights.
- **Proposal data** $\mathcal{D}_{\text{prop}}$: fresh samples from π_t , used to estimate the normalization constant $\psi(\beta)$.

We construct a grid G of candidate β values from the observed likelihood ratios across both datasets:

$$G = \text{PREPAREGRID}(\{\text{LR}(x) : x \in \mathcal{D}_{\text{cal}} \cup \mathcal{D}_{\text{prop}}\}). \quad (48)$$

The grid is sorted in increasing order, and we search from the most conservative (smallest β) to the most permissive, stopping at the first β where the weighted infeasibility rate exceeds α . See Figure 7 for an illustration.

C.1.2. ESTIMATING THE NORMALIZATION CONSTANT $\psi(\beta)$

Recall that the constrained policy is defined as

$$\pi^{(\beta)}(x) = \frac{\min\{\pi_t(x), \beta \cdot \pi_0(x)\}}{\psi(\beta)}, \quad (49)$$

where $\psi(\beta) = \int \min\{\pi_t(x), \beta \cdot \pi_0(x)\} dx$ is the normalization constant. We estimate $\psi(\beta)$ via importance-weighted Monte Carlo integration using the proposal data $\mathcal{D}_{\text{prop}}$.

When sampling from the optimistic policy π_t :

$$\psi(\beta) = \mathbb{E}_{\pi_t} \left[\frac{\min\{\pi_t(x), \beta \cdot \pi_0(x)\}}{\pi_t(x)} \right] = \mathbb{E}_{\pi_t} \left[\min \left\{ \frac{\beta}{\text{LR}(x)}, 1 \right\} \right] \quad (50)$$

$$\approx \frac{1}{|\mathcal{D}_{\text{prop}}|} \sum_{x \in \mathcal{D}_{\text{prop}}} \min \left\{ \frac{\beta}{\text{LR}(x)}, 1 \right\}. \quad (51)$$

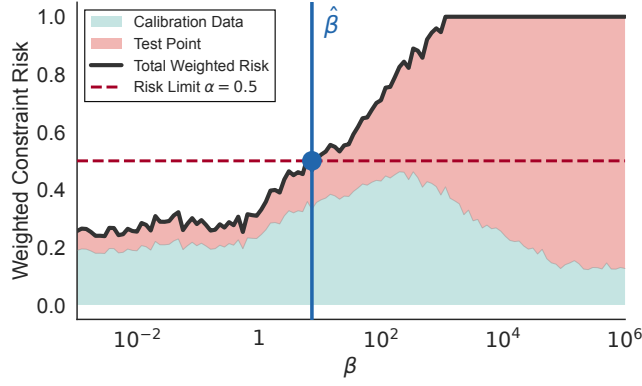


Figure 7. An illustration of fitting $\hat{\beta}$ to calibration data drawn from π_0 . We draw a test point from the optimized policy and conservatively assume the loss attains the upper bound B . As β increases, the contribution of the test point to the weighted average constraint violation increases. We search β in increasing order, recomputing the conformal weights for each setting of β and halting at the first point $\hat{\beta}$ where the average constraint violation exceeds α .

When sampling from the safe policy π_0 :

$$\psi(\beta) = \mathbb{E}_{\pi_0} \left[\frac{\min\{\pi_t(x), \beta \cdot \pi_0(x)\}}{\pi_0(x)} \right] = \mathbb{E}_{\pi_0} [\min\{\text{LR}(x), \beta\}] \quad (52)$$

$$\approx \frac{1}{|\mathcal{D}_{\text{prop}}|} \sum_{x \in \mathcal{D}_{\text{prop}}} \min\{\text{LR}(x), \beta\}. \quad (53)$$

In practice, all computations are performed in log space for numerical stability. Writing $r_i = \log \text{LR}(x_i)$ for each sample, the log normalization constant is

$$\log \psi(\beta) = \text{logsumexp}(\{\min(\log \beta - r_i, 0)\}_{i=1}^n) - \log n \quad (54)$$

for the optimistic proposal, and similarly with $\min(r_i, \log \beta)$ for the safe proposal.

C.1.3. CONFORMAL WEIGHTING

The calibration data \mathcal{D}_{cal} is drawn from a mixture of policies across previous rounds. To apply conformal prediction under this distribution shift, we weight each calibration point by the likelihood ratio between the candidate constrained policy and the calibration mixture:

$$\tilde{w}_i(\beta) = \frac{\pi^{(\beta)}(x_i)}{\pi_{\text{mix}}(x_i)}, \quad x_i \in \mathcal{D}_{\text{cal}}, \quad (55)$$

where π_{mix} is the mixture distribution over previous constrained policies, weighted by the number of calibration samples from each round.

For the test point, we use a conservative upper bound by taking the maximum weight over the proposal samples:

$$\tilde{w}_{\text{test}}(\beta) = \max_{x \in \mathcal{D}_{\text{prop}}} \frac{\pi^{(\beta)}(x)}{\pi_{\text{mix}}(x)}. \quad (56)$$

We normalize all weights to sum to one:

$$w_i(\beta) = \frac{\tilde{w}_i(\beta)}{\sum_j \tilde{w}_j(\beta) + \tilde{w}_{\text{test}}(\beta)}, \quad w_{\text{test}}(\beta) = \frac{\tilde{w}_{\text{test}}(\beta)}{\sum_j \tilde{w}_j(\beta) + \tilde{w}_{\text{test}}(\beta)}. \quad (57)$$

Let B denote the upper bound on the loss $\ell(x)$. The weighted risk estimate is

$$\hat{R}(\beta) = \sum_{i \in \mathcal{D}_{\text{cal}}} w_i(\beta) \ell(x_i) + w_{\text{test}}(\beta) \cdot B, \quad (58)$$

where the test point is conservatively assigned the worst-case loss B . We select $\hat{\beta}$ as the largest value in the grid G such that $\hat{R}(\beta) \leq \alpha$.

C.2. Sampling from the Constrained/Risk-Controlling Policy

In this section, we describe three approaches to sample from $\pi^{(\beta)}$: rejection sampling with either π_0 or π_t as the proposal (Section C.2.1), rejection sampling with a mixture proposal (Section C.2.2), and Independence Metropolis-Hastings (Section C.2.3).

C.2.1. REJECTION SAMPLING WITH SIMPLE PROPOSALS

We first review the classic accept-reject procedure. Let $\tilde{p}(x)$ be an unnormalized target density and $q(x)$ a normalized proposal such that

$$\frac{\tilde{p}(x)}{q(x)} \leq M \quad \forall x,$$

for some envelope constant $M < \infty$.⁹ To sample from $p(x) = \tilde{p}(x) / \int \tilde{p}(x) dx$, we proceed as follows: draw $X \sim q$, draw $U \sim \text{Unif}(0, 1)$, and accept X if $U \leq \frac{\tilde{p}(X)}{Mq(X)}$. The optimal (smallest) envelope constant is

$$M^* = \sup_x \frac{\tilde{p}(x)}{q(x)}.$$

The marginal acceptance probability is

$$\begin{aligned} \mathbb{P} \left[U \leq \frac{\tilde{p}(X)}{Mq(X)} \right] &= \mathbb{E} \left[\mathbb{1} \left\{ U \leq \frac{\tilde{p}(X)}{Mq(X)} \right\} \right] \\ &= \mathbb{E} \left[\mathbb{E} \left[\mathbb{1} \left\{ U \leq \frac{\tilde{p}(X)}{Mq(X)} \right\} \mid X \right] \right] \\ &= \mathbb{E} \left[\mathbb{P} \left[U \leq \frac{\tilde{p}(X)}{Mq(X)} \mid X \right] \right] \\ &= \mathbb{E}_{X \sim q} \left[\frac{\tilde{p}(X)}{Mq(X)} \right] \\ &= \int_{x:q(x)>0} q(x) \frac{\tilde{p}(x)}{Mq(x)} dx \\ &= \frac{1}{M} \int_{x:q(x)>0} \tilde{p}(x) dx \end{aligned} \tag{59}$$

so tighter M leads to higher acceptance rates.

Safe policy proposal. Take $\tilde{p}(x) = \tilde{\pi}^{(\beta)}(x) = \min\{\pi_t(x), \beta\pi_{\text{safe}}(x)\}$ and $q(x) = \pi_{\text{safe}}(x)$. Then for all x ,

$$\frac{\tilde{p}(x)}{q(x)} = \min \left\{ \frac{\pi_t(x)}{\pi_{\text{safe}}(x)}, \beta \right\} \leq \beta,$$

so we choose $M = \beta$. The pointwise acceptance probability then is

$$\frac{\tilde{p}(x)}{\beta\pi_{\text{safe}}(x)} = \min \left\{ \frac{\pi_t(x)}{\beta\pi_{\text{safe}}(x)}, 1 \right\}, \tag{60}$$

or $\frac{\pi_t(x)}{\beta\pi_{\text{safe}}(x)}$ in the unclipped region and 1 in the clipped region.

⁹Alternatively, we can view $Mq(x)$ as the unnormalized envelope proposal with normalizing constant M .

Optimized policy proposal. If we instead take $q(x) = \pi_t(x)$, then for all x ,

$$\frac{\tilde{p}(x)}{q(x)} = \frac{\min\{\pi_t(x), \beta\pi_{\text{safe}}(x)\}}{\pi_t(x)} = \min\left\{1, \frac{\beta\pi_{\text{safe}}(x)}{\pi_t(x)}\right\} \leq 1,$$

so we may take $M = 1$. The pointwise acceptance probability is

$$\frac{\tilde{p}(x)}{\pi_t(x)} = \min\left\{1, \frac{\beta\pi_{\text{safe}}(x)}{\pi_t(x)}\right\}, \quad (61)$$

which is 1 in the unclipped region and $\frac{\beta\pi_{\text{safe}}(x)}{\pi_t(x)}$ in the clipped region.

Intuitively, the relative efficiency of the two proposals depends on the constraint parameter β controlling how much the optimized policy is truncated toward the safe policy. When β is small, the constrained target resembles a rescaled version of π_{safe} over most of its support. Proposing from π_{safe} tends to be efficient in this regime, because most points satisfy $\pi_t(x)/\pi_{\text{safe}}(x) \ll \beta$ and the acceptance probability in Equation 60, while small, varies smoothly over x . In contrast, proposing from π_t can be inefficient with small β , since π_t may place substantial mass in regions that are heavily downweighted by the constraint, leading to frequent rejections.

When β is large, the constrained target resembles π_t . As long as $\pi_t(x)/\pi_{\text{safe}}(x) \lesssim \beta$ for most of the support of π_t , then using π_t as the proposal tends to be more efficient in this regime, as the acceptance probability in Equation 61 is frequently close to 1. If, however, π_t concentrates mass in regions where $\pi_t(x)/\pi_{\text{safe}}(x)$ is extremely large, this proposal can still perform poorly.

At intermediate values of β , neither proposal dominates. The constrained target may allocate comparable mass from π_{safe} and π_t . Both proposals can suffer from mismatches with different parts of the target, motivating the use of mixture proposals that adaptively trade off between π_{safe} and π_t .

C.2.2. REJECTION SAMPLING WITH MIXTURE PROPOSAL

Let the proposal be the mixture

$$q_w(x) = w\pi_{\text{safe}}(x) + (1-w)\pi_t(x), \quad w \in [0, 1].$$

The tight envelope constant is

$$M^*(w) = \sup_x \frac{\tilde{p}(x)}{q_w(x)} = \sup_x \frac{\min\{\pi_t(x), \beta\pi_{\text{safe}}(x)\}}{w\pi_{\text{safe}}(x) + (1-w)\pi_t(x)}.$$

Given any $M \geq M^*(w)$, the pointwise acceptance probability is

$$\alpha_w(x) := \frac{\tilde{p}(x)}{Mq_w(x)} = \frac{\min\{\pi_t(x), \beta\pi_{\text{safe}}(x)\}}{M(w\pi_{\text{safe}}(x) + (1-w)\pi_t(x))}. \quad (62)$$

Choosing smaller M (i.e., closer to M^*) yields higher acceptance rates, as derived in Equation 59. In practice, we may choose M by estimating $M^*(w)$ from a set of points \mathcal{S} covering the support of q_w , where \mathcal{S} is obtained by drawing samples from q_w or some appropriate fraction of samples from each component to cover the tails. Taking the empirical maximum

$$\max_{x \in \mathcal{S}} \frac{\tilde{p}(x)}{q_w(x)}$$

then yields an estimate of $M^*(w)$.

We now describe a few simple methods for choosing w .

Joint grid search with M . We can iterate over a grid of w and choose w, M jointly. For each candidate value of w , estimate $M^*(w)$ using the procedure described above and choose w that minimizes this estimate. Note that the support points \mathcal{S} used to estimate $M^*(\cdot)$ can be reused for different values of w .

Estimated overlap coefficients. The *overlap coefficient* between two density functions p_1, p_2 is defined as

$$\text{OVL}(p_1, p_2) := \int \min \{p_1(x), p_2(x)\} dx = \int \min \left\{ \frac{p_1(x)}{p_2(x)}, 1 \right\} p_2(x) dx \in [0, 1].$$

It is related to the total variation (TV) distance as $\text{OVL}(p_1, p_2) = 1 - \text{TV}(p_1, p_2)$.

Letting $p_1 = p = \pi^{(\beta)}$, our normalized target, we can estimate $\text{OVL}(\pi^{(\beta)}, \pi_{\text{safe}})$ using samples x_1, \dots, x_n drawn from π_{safe} :

$$\widehat{\text{OVL}}(\pi^{(\beta)}, \pi_{\text{safe}}) = \frac{1}{n} \sum_{i=1}^n \min \left\{ \frac{\pi^{(\beta)}(x_i)}{\pi_{\text{safe}}(x_i)}, 1 \right\} = \frac{1}{n} \sum_{i=1}^n \min \left\{ \frac{\pi_t(x_i)}{\psi(\beta)\pi_{\text{safe}}(x_i)}, \frac{\beta}{\psi(\beta)}, 1 \right\}, \quad (63)$$

and similarly $\widehat{\text{OVL}}(\pi^{(\beta)}, \pi_t)$ using samples drawn from π_t . The normalizing constant $\psi(\beta)$ is estimated with importance-weighted MC integration as described in Section C.1.2. A simple heuristic is then to set

$$w = \frac{\widehat{\text{OVL}}(\pi^{(\beta)}, \pi_{\text{safe}})}{\widehat{\text{OVL}}(\pi^{(\beta)}, \pi_{\text{safe}}) + \widehat{\text{OVL}}(\pi^{(\beta)}, \pi_t)}. \quad (64)$$

This chooses the mixture weights proportional to each component's estimated overlap with the target, biasing the proposal toward whichever component more closely matches the constrained policy, while retaining support from both.

Adaptive update. Rather than fixing w , we can adapt it online in the direction of a desirable sampling diagnostic. For example, we might define an update based on the observed acceptance rates of proposals drawn from each component, so that w shifts toward the component that yields higher acceptance.

C.2.3. INDEPENDENCE METROPOLIS-HASTINGS SAMPLING

While rejection sampling yields exact samples from the target distribution, it requires finding a finite global bound M satisfying $\tilde{p}(x)/q(x) \leq M$ for all x . In many settings, especially in high dimensions, this bound is too loose to be practical or may not exist at all. The Metropolis-Hastings algorithm (Metropolis et al., 1953; Hastings, 1970) relaxes this requirement. In particular, here we discuss a simple variant called the independence Metropolis Hastings (IMH) algorithm, where the proposal does not depend on the current state (Tierney, 1994).

Given an unnormalized target $\tilde{p}(x)$ and a normalized proposal $q(x)$, we initialize the Markov chain at x_0 and the IMH algorithm evolves it as follows. From the current state x_t , draw a candidate state $x' \sim q$, compute the acceptance probability

$$a(x', x_t) = \min \left\{ 1, \frac{r(x')}{r(x_t)} \right\}, \quad r(x) := \frac{\tilde{p}(x)}{q(x)},$$

draw $U \sim \text{Unif}(0, 1)$, and accept x' (i.e., set $x_{t+1} = x'$) if $U \leq a(x', x_t)$ otherwise copy the old state $x_{t+1} = x_t$. It can be shown that the invariant distribution of the resulting Markov chain $x_0, x_1, x_2 \dots$ is the target $p(x)$. Intuitively, IMH compares each proposal only to the current state, whereas rejection sampling compares each proposal to a global worst case.

D. Medical QA Implementation Details and Additional Results

This appendix provides implementation details for our medical question-answering experiments, connecting the general conformal risk control framework to the specific problem of controlling LLM factuality. We describe the problem setup and notation (Section D.1), prior approaches to conformal factuality (Section D.2), loss functions for factuality control including the non-monotonic FDR loss (Section D.3), experimental setup (Section D.4), and hyperparameters (Section D.5).

D.1. Problem Setup and Notation

Following [Mohri & Hashimoto \(2024\)](#) and [Cherian et al. \(2024\)](#), we formalize the natural language factuality setting as follows. Each data sample Z_i is a prompt-response-claim-annotation tuple:

$$Z_i := (X_i, X'_i, \mathbf{C}_i, \mathbf{Y}_i), \quad (65)$$

where X_i is the prompt (question), X'_i is the full LLM response, $\mathbf{C}_i = (C_{i1}, \dots, C_{ik_i})$ is the vector of atomic subclaims extracted from X'_i , and $\mathbf{Y}_i = (Y_{i1}, \dots, Y_{ik_i})$ contains binary annotations indicating whether each subclaim is factually correct ($Y_{ij} = 1$) or incorrect ($Y_{ij} = 0$).

For each subclaim C_{ij} , let $p(C_{ij} | X_i) \in [0, 1]$ denote a prompt-conditional confidence score estimating the likelihood that the subclaim is factual. Higher scores indicate greater confidence in factuality.

D.2. Prior Approaches to Conformal Factuality

Mohri & Hashimoto (2024). [Mohri & Hashimoto \(2024\)](#) achieve conformal factuality guarantees by filtering subclaims based on a threshold τ determined by split conformal prediction. A subclaim C_{ij} is included in the filtered response if $p(C_{ij} | X_i) \geq \tau$. The corresponding non-conformity score for each response is the smallest threshold such that all included subclaims are factual:

$$s(Z_i) = \inf \{ \tau : Y_{ij} = 1 \text{ for all } j \text{ with } p(C_{ij} | X_i) \geq \tau \}. \quad (66)$$

The threshold $\hat{\tau}$ is then selected as the $(1 - \alpha)$ -quantile of the calibration scores:

$$\hat{\tau} = \inf \left\{ \tau : \frac{1}{n} \sum_{i=1}^n \mathbb{1}\{s(Z_i) \leq \tau\} \geq \frac{\lceil (n+1)(1-\alpha) \rceil}{n} \right\}. \quad (67)$$

Cherian et al. (2024). [Cherian et al. \(2024\)](#) extend this approach using conditional calibration and multicalibration to provide guarantees that hold across different subgroups of prompts, addressing the limitation that marginal guarantees may not hold uniformly across topics or question types.

D.3. Loss Functions for Factuality Control

Binary indicator loss (prior work). The loss function implicitly used by [Mohri & Hashimoto \(2024\)](#) and [Cherian et al. \(2024\)](#) is the binary indicator for whether any included subclaim is incorrect:

$$L_i^{\text{binary}}(\tau) = \mathbb{1}\left\{ \exists j : p(C_{ij} | X_i) \geq \tau \text{ and } Y_{ij} = 0 \right\}. \quad (68)$$

Controlling this loss at level α guarantees $\mathbb{P}(\text{any included claim is false}) \leq \alpha$. This loss is monotonically non-increasing in τ by construction: as the threshold increases, fewer claims are included, so the probability of including a false claim can only decrease.

False discovery rate loss (this work). We instead use a more granular loss: the false discovery rate (FDR), *i.e.*, the fraction of included subclaims that are false:

$$L_i(\tau) = \frac{\sum_{j=1}^{k_i} (1 - Y_{ij}) \cdot \mathbb{1}\{p(C_{ij} | X_i) \geq \tau\}}{\underbrace{\sum_{j=1}^{k_i} \mathbb{1}\{p(C_{ij} | X_i) \geq \tau\}}_{\text{FDR}_i(\tau) = 1 - \text{Precision}_i(\tau)}}, \quad (69)$$

with $L_i(\tau) = 0$ when no claims are included. This is precisely $1 - \text{Precision}_i(\tau)$, where precision is the fraction of included claims that are true. Controlling this loss at level α ensures:

$$\mathbb{E}[\text{FDR}_i(\tau)] \leq \alpha \iff \mathbb{E}[\text{Precision}_i(\tau)] \geq 1 - \alpha. \quad (70)$$

Why FDR control requires generalized CRC. Unlike the binary loss, the FDR loss in (69) is not monotonic in τ . As τ increases, both the numerator (false claims included) and denominator (total claims included) decrease, but not necessarily at the same rate. This non-monotonicity means standard CRC (Angelopoulos et al., 2024) does not apply directly, motivating our generalized CRC approach.

For methods requiring monotonicity, one can use the monotonized loss:

$$\tilde{L}_i(\tau) = \sup_{\tau' \geq \tau} L_i(\tau'), \quad (71)$$

which upper-bounds the FDR and is monotonically non-increasing by construction. However, this monotonization can be overly conservative.

Reward metric: true claim recall. While we control the FDR (our loss), we measure the recall of true claims as our reward metric:

$$\text{Recall}_i(\tau) = \frac{\sum_{j:Y_{ij}=1} \mathbb{1}\{p(C_{ij} | X_i) \geq \tau\}}{\sum_{j=1}^{k_i} Y_{ij}}, \quad (72)$$

i.e., the fraction of true subclaims that are retained after filtering. For a given FDR target α , methods that achieve higher recall preserve more useful information while satisfying the same safety constraint.

D.4. Experimental Setup

Our experimental setup closely follows Cherian et al. (2024), with the key modification of controlling the FDR loss (69) and measuring recall (72) as a reward metric.

D.4.1. DATASET

We use the **MedLFQA** (Medical Long-Form Question Answering) dataset from Jeong et al. (2024), which aggregates four established medical QA benchmarks:

- **HealthSearchQA** ($n = 3047$): Consumer health questions
- **K-QA** ($n = 1077$): Knowledge-intensive medical questions, with a subset having gold-standard physician responses (K-QA Golden, $n = 201$) and the remainder having LLM-generated responses (K-QA Silver)
- **LiveQA** ($n = 100$): Real consumer health questions from the National Library of Medicine
- **MedicationQA** ($n = 627$): Questions about medications and drug interactions

Each prompt is accompanied by either an LLM or human-generated reference response, which serves as ground truth for evaluating factual accuracy.

D.4.2. DATA GENERATION PIPELINE

We use the annotated dataset from Cherian et al. (2024), which was constructed through a three-stage pipeline:

1. **Response generation:** GPT-3.5-Turbo was queried with each medical question to obtain a candidate response X'_i .
2. **Subclaim extraction:** GPT-4o parsed each response into atomic subclaims $C_i = (C_{i1}, \dots, C_{ik_i})$.
3. **Factuality annotation:** GPT-3.5-Turbo evaluated whether each subclaim is substantiated by the reference response, yielding binary annotations $Y_{ij} \in \{0, 1\}$.

For subclaim scoring, we use **self-evaluation scores** $p(C_{ij} | X_i)$, where the LLM is prompted to assess its own confidence in each claim.

D.4.3. METHODS COMPARED

We compare three conformal risk control methods:

- **GCRC (proposed)**: Generalized conformal risk control as described in Section 4, which searches thresholds from safest to most aggressive and stops when the augmented empirical risk exceeds α .
- **Monotonized-losses CRC** (Angelopoulos et al., 2024; Mohri & Hashimoto, 2024): Applies standard CRC to the monotonized loss $\tilde{L}_i(\tau) = \sup_{\tau' \geq \tau} L_i(\tau')$, which upper-bounds the FDR.
- **Learn Then Test (LTT)** (Angelopoulos et al., 2025): A multiple testing approach using Hoeffding-Bentkus p -values to identify valid thresholds with family-wise error rate control. Unlike CRC methods, LTT does not add a conservative test-point loss term.

D.4.4. EXPERIMENTAL PROTOCOL

- **Calibration/test split**: 70%/30% random split of the dataset
- **Risk levels**: $\alpha \in \{0.005, 0.01, 0.015, \dots, 0.10\}$ (20 values)
- **Threshold grid**: 200 candidate thresholds sampled from the empirical distribution of subclaim scores
- **Random seeds**: Results averaged over 10 independent train/test splits
- **Score jittering**: Uniform noise ($\sim 10^{-8}$) added to break ties

D.5. Hyperparameters

Table 2 summarizes the experimental configuration.

Table 2. Hyperparameters for medical QA experiments.

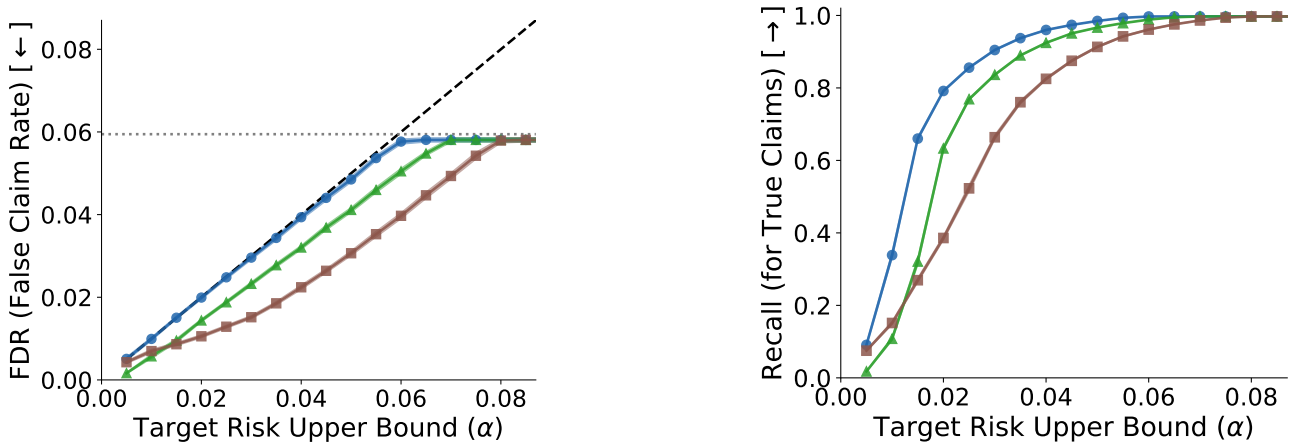
Parameter	Symbol	Value
Calibration fraction	–	0.7
Number of trials	–	10
Threshold grid size	$ \Lambda $	200
Risk levels tested	α	$\{0.005, 0.01, \dots, 0.10\}$
Score jitter magnitude	–	10^{-8}
Response LLM	–	GPT-3.5-Turbo
Subclaim extraction LLM	–	GPT-4o
Annotation LLM	–	GPT-3.5-Turbo
Subclaim scoring method	–	Self-evaluation

D.6. Additional Medical QA Results

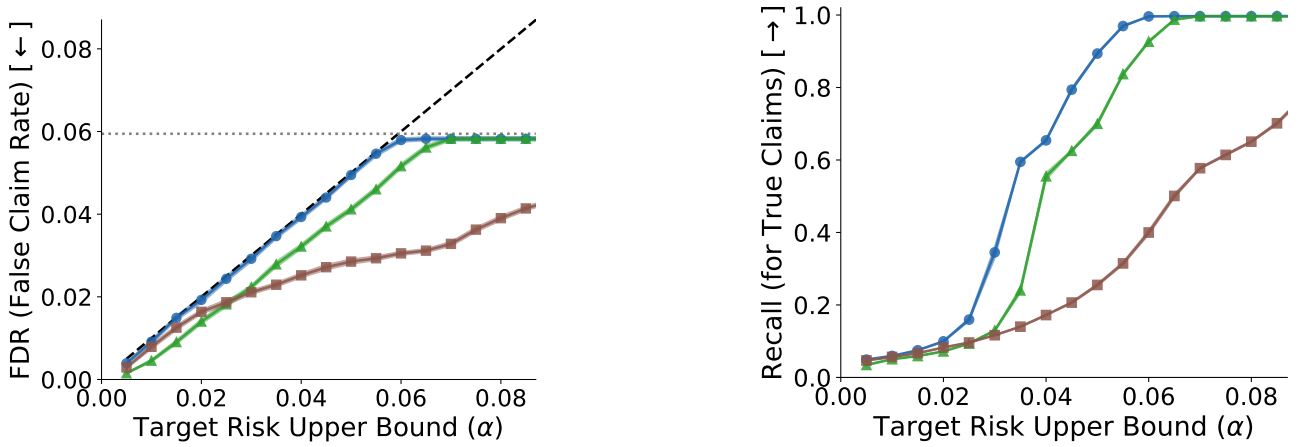
Conformal Policy Control

-- Target Risk Upper Bound
 ⋯ Population Avg. Risk
 ● GCRC (proposed)
 ▲ LTT (Angelopoulos, et al., 2025)
 ■ Monotized-losses CRC (Mohri & Hashimoto, 2024; Angelopoulos et al., 2024)

Log-Probabilities Subclaim Scoring



Self-Evaluation Subclaim Scoring



Frequency Subclaim Scoring

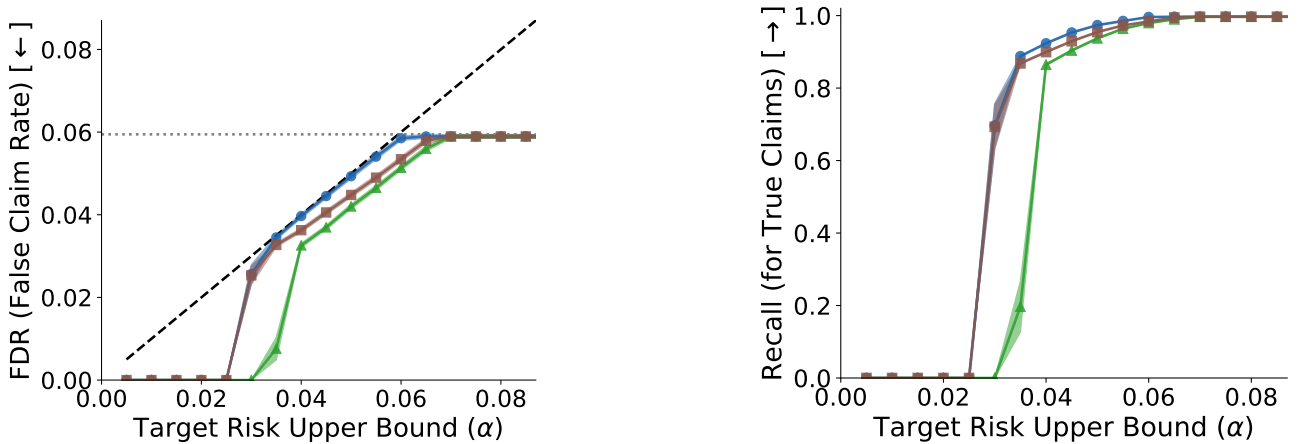


Figure 8. Medical QA factuality control results on MedLFQA on three subclaim scoring methods: log-probabilities (**top row**), self-evaluation (**middle row**), and frequency (**bottom row**). **Left column:** Empirical FDR (fraction of retained claims that are false) vs. target risk level α . The black dashed line indicates $y = x$; valid methods should fall at or below this line. **Right column:** Recall (fraction of true claims retained) vs. α . gCRC tightly controls FDR at the target level while achieving superior recall to baselines. Results averaged over 25 random splits. Error regions are standard errors.

E. Constrained Tabular Active Learning Implementation Details and Additional Results

This appendix provides implementation details for the constrained active learning experiments in Section 5.2. We describe the datasets used for evaluation (Section E.1), the construction of synthetic feasibility constraints based on principal component analysis (Section E.2), the active learning setup including surrogate model and acquisition policy (Section E.3), and hyperparameter settings (Section E.4).

E.1. Datasets

We evaluate on three regression datasets:

- **Robot Arm Kinematics** (University of Toronto, 1996) (8192 samples, 8 features): Predict end-effector distance from joint angles of an 8-link all-revolute robot arm. We use the kin8nm variant from the DELVE repository, a highly non-linear regression task with moderate noise.
- **Airfoil Self-Noise** (Brooks et al., 1989) (1503 samples, 5 features): Predict sound pressure level from aerodynamic and geometric properties of NACA 0012 airfoil blade sections tested in an anechoic wind tunnel. We apply log transforms to frequency and suction-side displacement thickness following standard practice.
- **Medical Expenditure Panel Survey (Medical Utilization or MEPS)** (Ezzati-Rice et al., 2008) (33005 samples, 107 features): Large-scale survey dataset on medical utilization and costs of health care and health insurance coverage. Surveys are of individuals and families, their medical providers, and employers across the United States. We pre-process the data (for instance constructing dummy/indicator covariates) as described in Barber et al. (2021). Data available at https://meps.ahrq.gov/mepsweb/data_stats/download_data_files_detail.jsp?cboPufNumber=HC-192

E.2. Feasibility Constraint Construction

Our datasets do not include recorded feasibility constraints, so we construct synthetic constraints based on the first principal component of the covariate matrix. The first principal component captures the dominant pattern of covariation in the data. Records with high PC1 values follow this typical covariation pattern and are likely feasible, while records with low PC1 values deviate from this pattern. Their covariates vary in an atypical or “weird” way that we treat as risky. This captures the intuition that unusual configurations are more likely to violate constraints.

We define the feasibility indicator for each record as follows:

1. **PCA projection:** Compute the first principal component of the full covariate matrix $X \in \mathbb{R}^{n \times d}$ and project all records onto this axis, yielding $z_i \in \mathbb{R}$ for each record i .
2. **Exponential tilting:** Apply min-max normalization to $\{z_i\}$ and compute exponentially-tilted values $\tilde{z}_i = \exp(\gamma \cdot z_i^{\text{norm}})$, where $\gamma > 0$ is the `initial_sampling_bias` parameter.
3. **Feasibility probability:** Convert relative ranks of $\{\tilde{z}_i\}$ to feasibility probabilities via a logistic CDF:

$$p_i^{\text{feasible}} = \sigma\left(\text{rank}(\tilde{z}_i)/n; \mu, s\right), \quad (73)$$

where $\sigma(\cdot; \mu, s)$ is the logistic CDF with location $\mu = \min(2.5\alpha, 0.98)$, scale $s = 0.1$, and α is the target risk level for CPC. We tie the logistic location to α so that the proportion of infeasible records in the pool scales with the target risk level, ensuring the constraint remains binding across different choices of α . For our experiments with $\alpha = 0.2$, this yields $\mu = 0.5$.

4. **Bernoulli sampling:** Sample feasibility indicators $F_i \sim \text{Bernoulli}(p_i^{\text{feasible}})$.

The initial training data is sampled with the same exponential tilting toward high PC1 values (Section E.3), so the learner begins in a high-feasibility region where covariates follow the dominant covariation pattern. The pool contains many records from the opposite end of the PC1 spectrum, atypical configurations with low feasibility probability that a naive uncertainty-based acquisition policy would preferentially select.

E.3. Active Learning Setup

Initial data. We hold out 20% of each dataset as a fixed test set for evaluating MSE. From the remaining records, we sample n_{initial} points with exponential tilting toward high PC1 values (using the same bias parameter γ from Section E.2), then split these into training (80%) and calibration (20%) sets. This biased initialization places the learner in the high-feasibility region where covariates follow typical covariation patterns, reflecting a scenario where the incumbent safe policy operates in well-understood regimes.

Surrogate model. We fit a Gaussian Process (GP) regression model with a DotProduct + WhiteKernel covariance function using the `scikit-learn` package (Pedregosa et al., 2011):

$$k(x, x') = \sigma_0^2 + x^\top x' + \sigma_n^2 \cdot \mathbf{1}[x = x'], \tag{74}$$

where σ_0^2 is the signal variance and σ_n^2 is the noise variance.

Acquisition policy. At each iteration, we define an acquisition distribution over pool records via exponential tilting toward posterior variance. The action $a \in \mathcal{A}_t$ is an index into the pool of unlabeled records at iteration t , and the acquisition policy is

$$\pi(a) \propto \exp\left(\lambda \cdot \frac{\hat{\sigma}_a^2}{\max_{j \in \mathcal{A}_t} \hat{\sigma}_j^2 - \min_{j \in \mathcal{A}_t} \hat{\sigma}_j^2}\right), \tag{75}$$

where $\hat{\sigma}_a^2$ is the posterior variance of the latent function f (not the noisy labels y) at the covariates for record a , and $\lambda > 0$ controls the degree of uncertainty-seeking behavior. This policy preferentially selects records where the model is uncertain, which in our setup corresponds to regions with atypical covariation patterns (and thus potentially infeasible).

Conformal policy control. Before sampling, we apply CPC to constrain the acquisition policy relative to the initial source distribution (the biased sampling distribution used for initialization). This clips the likelihood ratio between the acquisition policy and source policy, as described in Section 4.2, to control the risk of selecting infeasible records.

Sequential updates. At each iteration, we sample one record from the (constrained) acquisition policy with replacement (the pool remains unchanged), observe a noisy version of its label (Gaussian noise with magnitude 0.05) and its feasibility indicator, and add the observation to either the training or calibration set with equal probability. The GP is then refit on the updated training set. We repeat this process for T iterations.

E.4. Hyperparameters

Table 3 summarizes the hyperparameters used in our experiments.

Table 3. Hyperparameters for constrained active learning experiments.

Parameter	Symbol	Value
Initial pool size	n_{initial}	48
Initial train/cal split	–	80%/20%
Acquisition iterations	T	10
New point train probability	–	0.5
Sampling bias	γ	1.0
Acquisition temperature	λ	10.0
GP signal variance	σ_0^2	1.0
GP noise variance	σ_n^2	1.0
Observation noise magnitude	–	0.05
Target risk level	α	0.2

F. Constrained Black-Box Sequence Optimization Implementation Details and Results

This appendix provides implementation details for the constrained black-box sequence optimization experiments in Section 5.3. We describe the Ehrlich test functions used for evaluation (Section F.1), the procedure for training the safe policy via supervised fine-tuning on genetic algorithm data (Section F.2), the policy improvement procedure via DPO (Section F.3), and supplementary results across additional risk levels (Figure 9).

F.1. Ehrlich Test Functions

We evaluate CPC on Ehrlich functions (Chen et al., 2025), a class of synthetic test functions designed to capture the geometric structure of biomolecular sequence optimization problems such as antibody affinity maturation. An Ehrlich function $f : \mathcal{V}^L \rightarrow (-\infty, 1]$ maps sequences of length L over a vocabulary \mathcal{V} to a score indicating how well the sequence satisfies a collection of c gapped motifs $\mathbf{m}^{(i)}$ with spacing $\mathbf{s}^{(i)}$. Formally,

$$f(\mathbf{x}) = \begin{cases} \prod_{i=1}^c g \circ h_q(\mathbf{x}, \mathbf{m}^{(i)}, \mathbf{s}^{(i)}) & \text{if } \mathbf{x} \in \mathcal{F} \\ -\infty & \text{otherwise} \end{cases}, \quad (76)$$

where h_q measures motif satisfaction with precision q , g is a response function capturing epistatic effects, and \mathcal{F} is a feasibility set defined by a discrete Markov process with certain infeasible transitions (*i.e.* some bigrams have zero probability mass). Sequences outside \mathcal{F} are assigned $-\infty$, modeling expression constraints in real biophysical assays.

We follow the naming convention **Ehr**($|\mathcal{V}|, L$)- c - k - q from Chen et al. (2025), where k is the motif length and q controls signal sparsity. Ehrlich functions are procedurally generated, have adjustable difficulty, and are provably solvable, making them well-suited for benchmarking constrained optimization algorithms. In our experiments, we use **Ehr(32, 32)-4-4-4**: sequences of length $L = 32$ over a vocabulary of size $|\mathcal{V}| = 32$, with $c = 4$ motifs of length $k = 4$ and quantization precision $q = 4$.

F.2. Training the Safe Policy

Following Chen et al. (2025), we initialize the optimization loop with a data package $\mathcal{D}^{(0)}$ collected from a genetic algorithm (GA) pre-solver. Starting from a single feasible seed sequence \mathbf{x}_0 sampled from the discrete Markov process, we run $n_0 = 10$ rounds of the GA with 5000 particles per iteration. This produces approximately 50K scored sequences that provide initial coverage of the feasible region \mathcal{F} . The GA uses mutation probability $p_m = 0.05$ and survival quantile $\alpha = 0.5$.

From the GA history, we construct the initial supervised fine-tuning (SFT) dataset by identifying improving pairs: for each sequence \mathbf{x} in the history, we search for sequences \mathbf{x}' within edit distance δ such that $f(\mathbf{x}') > f(\mathbf{x})$. These $(\mathbf{x}, \mathbf{x}')$ pairs form instruction-response examples for training the safe policy π_{θ_0} , which we initialize from a Pythia 14M-parameter decoder-only transformer (Biderman et al., 2023). See Table 4 for hyperparameter settings.

Table 4. Hyperparameters for training the safe policy via SFT.

Hyperparameter	Value
Base model	Pythia 14M
Learning rate	10^{-6}
Training epochs	10
Batch size	32
Edit distance threshold (δ)	$0.3 \cdot L$

F.3. Improving the Safe Policy

To improve the safe policy, we take a fixed set of seed sequences from the GA optimizer history and sample actions from π_{θ_0} . From the resulting data, we construct DPO preference triplets of the form $(\mathbf{x}, \mathbf{x}^+, \mathbf{x}^-)$, where \mathbf{x}^+ is preferred over \mathbf{x}^- based on the oracle scores. We initialize the improved policy π_{θ_t} at the safe policy weights and train using the DPO loss (Rafailov et al., 2023). See Algorithm 2 for pseudocode of a single round of CPC.

We chose DPO as our policy improvement method because Chen et al. (2025) demonstrated that it struggles with poor

Algorithm 2 Conformal Policy Control

Require: Safe policy π_0 ; context draws $\{X_i\}_{i=1}^n \sim p(X)$; target risk level α

Phase 1: Safe Policy Data Collection

Draw actions $A_i \sim \pi_0(\cdot | X_i)$ for $i = 1, \dots, n$

Observe rewards $R_i = r(X_i, A_i)$ and losses $L_i = \ell(X_i, A_i)$

Split data: $\mathcal{D}_{\text{train}}, \mathcal{D}_{\text{cal}} \leftarrow \text{RANDOMSPPLIT}(\{(X_i, A_i, R_i, L_i)\})$

Phase 2: Policy Improvement

$\pi_t \leftarrow \text{IMPROVEPOLICY}(\pi_0, \mathcal{D}_{\text{train}})$

Phase 3: Calibration

$\hat{\beta} \leftarrow \text{CALIBRATEBETA}(\pi_0, \pi_t, \mathcal{D}_{\text{cal}}, \alpha)$ (Algorithm 1)

Phase 4: Constrained Deployment

Draw improved actions $A'_i \sim \pi_t^{(\hat{\beta})}(\cdot | X_i)$ via accept-reject for $i = 1, \dots, n$

Return: $\{A'_i\}_{i=1}^n$

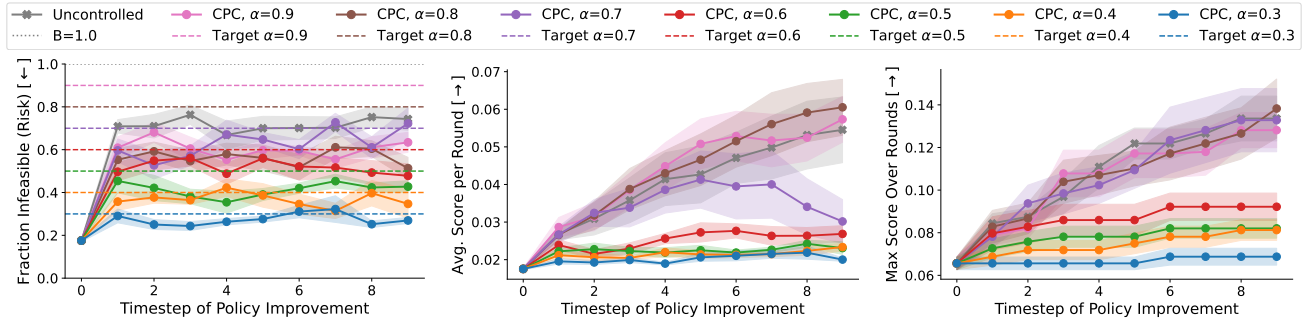


Figure 9. Supplementary experimental results applying CPC to constrained black-box optimization of token sequences scored with Ehrlich functions. In the **left** panel, we show the average feasibility rate round-over-round. In the **center**, we show the average objective value of solutions sampled from the DPO-tuned policy, and in the **right**, the best solution found so far at each round. CPC allows us to easily modify the constraint violation risk by directly manipulating α . We find that moderate risk control may actually stabilize the algorithm and lead to better overall performance since fewer samples are wasted to infeasibility constraints.

feasibility rates compared to other fine-tuning approaches, making it a challenging test case for our risk control procedure. See Table 5 for hyperparameter settings.

Table 5. Hyperparameters for policy improvement via DPO.

Hyperparameter	Value
Learning rate	10^{-7}
DPO β	0.4
Training epochs per round	1
Batch size	32
Number of DPO rounds	10